Physics – Uspekhi **49** (10) 1045 – 1065 (2006)

REVIEWS OF TOPICAL PROBLEMS PACS numbers: **52.80.–s**, 52.80.Dy, 52.80.Pi

Similarity laws for pulsed gas discharges

G A Mesyats

DOI: 10.1070/PU2006v049n10ABEH006118

Contents

Abstract. The feasibility of applying the similarity law to different types of pulsed discharges is analyzed. The analysis is based on the dependence $p\tau = f(E/p)$, where τ is the charge formation time, p is the gas pressure, and E is the pulsed field strength at which the breakdown occurs. The law holds for the Townsend and streamer breakdowns for a relatively long discharge gap d (for atmospheric air, $d > 1$ cm). For millimeter gaps, this law applies to many gases only in the case of the multielectron breakdown initiation down to the picosecond range. In this case, the time τ is measured from the instant the voltage amplitude sets in to the onset of current buildup and of the drop in voltage across the gap during the simultaneous development of a large number of electron avalanches. In the initiation by a small number of electrons, the time τ is longer than in the multielectron initiation by nearly an order of magnitude; this is due to the relatively low rate of free-electron accumulation in the gap, with runaway electrons (REs) playing an important role in this process. But the time θ of the fast voltage drop and current buildup obeys the similarity law $p\theta = F(E/p)$ in both cases. It is hypothesized that the source of REs is the field emission from cathodic micropoints, which terminates at the onset of explosive electron emission to limit the RE current pulse duration to 10^{-10} s. The similarity law $p\tau = f(E/p)$ is shown to hold for a pulsed microwave breakdown.

G A Mesyats Lebedev Physics Institute,
Russian Academy of Sciences,
Leninskii prosp. 53, 119991 Moscow, Russian Federation
Tel. (7-495) 135 24 30. Fax (7-495) 956 24 04
E-mail: mesyats@presidium.ras.ru

Received 12 May 2006
Uspekhi Fizicheskikh Nauk **176** (10) 1069 – 1091 (2006)
Translated by E N Ragozin; edited by A M Semikhatov

1. Introduction

1.1 General information

In the pursuance of electric gas discharge research, it is required to know the sort of gas, its pressure p and temperature T, the cathode – anode distance d (the gap length), the electrode radii R, the initial voltage U across the electrodes, etc. Measured in the course of investigations are the discharge voltage U and current i, the current density j, the electric intensity during discharge E, temporal characteristics t, etc. Furthermore, it is necessary to specify the distribution of all these quantities over the discharge space. When one characteristic is changed, having complete information about the discharge requires knowing how other characteristics change in this case. Owing to the complexity of functional connections between different parameters, a multitude of dependences are required to describe the discharge. That is why this approach to discharge research is practically unacceptable.

A substantial simplification can be made by grouping the quantities that characterize a discharge into certain combinations that describe one discharge property or another in a wide range of conditions. The significance of such grouping was already emphasized by Paschen and Townsend, who noted that the product of the electric field strength E and the electron mean free path λ expresses the energy gained by the electron over its mean free path and that the pressure p times the gap length d is proportional to the number of molecules between the electrodes. Consequently, when $E\lambda$ or E/p and pd are maintained constant, the electron multiplication in the gap is fixed. These and other parameter groups are required to study the behavior of the so-called similar discharges [1 – 4].

One condition that must be satisfied by similar discharges is that all linear dimensions be related as $1/a$, where a is a

constant quantity. This implies that the lengths d_1 and d_2 of two discharge gaps are related as $d_1 = ad_2$, the electrode radii are related as $R_1 = aR_2$, etc. Under these conditions, geometrically similar discharges occur. By completely similar discharges, we mean those that, apart from geometric similarity, are characterized by equal voltages $U_1 = U_2$ across the discharge gaps, equal discharge currents $i_1 = i_2$, and equal temperatures $T_1 = T_2$. Studying the behavior of geometrically similar discharges and investigating the conditions ensuring the complete similarity is of significance in designing the prototypes of large-scale facilities or in predicting discharge phenomena for very small dimensions, when direct measurements are hindered. On the other hand, proceeding from similarity laws allows drawing inferences about the occurrence of one elementary process or another in the discharge.

Proceeding from the definition of similar discharges, it is easy to relate their parameters via the constant a. The parameters used most frequently obey the relations given in Table 1. These relations permit making combinations that are invariant under the accepted transformation laws. This implies that these combinations have the same values in similar gaps and are, relative to other discharges, some universal parameters facilitating the discharge description. Among these combinations are Rp, E/p, pd, α/p, pt, j/p^2, f/p, and H/p. The current, the voltage, and the gas temperature are independent similarity parameters. The above similarity parameters are commonly employed for discharge characterization, and in many cases there exist unique relations between them, which are referred to as similarity laws.

The similarity laws for d.c. and continuous microwave discharges have been adequately studied [1 – 5]. The situation with pulsed discharges is much worse due to the diversity of pulsed discharge types. Especially numerous are the problems with nano- and picosecond discharges at high gas pressures, when the validity of similarity laws, like the validity of the Townsend classical theory in general, is called into question. In this review, we therefore briefly consider the origins of the similarity laws developed for stationary discharges and then investigate in greater detail the applicability of these laws to the temporal characteristics of different types of pulsed gas discharges.

Table 1.

Electrode surface area (e.g., discharge cross section)	$S_1 = a^2 S_2$
Volume	$V_1 = a^3 V_2$
Gas pressure	$p_1 = p_2/a$
Electric field strength	$E_1 = E_2/a$
Surface density of charge carriers	$\sigma_1 = \sigma_2/a$
Volume density of charge carriers	$n_1 = n_2/a^2$
Velocity of charge carriers	$v_1 = v_2$
Mobility	$\mu_1 = a\mu_2$
Discharge current density	$j_1 = j_2/a^2$
Collisional ionization coefficient	$\alpha_1 = \alpha_2/a$
Time interval	$\mathrm{d}t_1 = a\,\mathrm{d}t_2$
Collision frequency	$\nu_1 = \nu_2/a$
Mean free path of any particle	$\lambda_{01} = a\lambda_{02}$
Externally or current-produced magnetic field	$H_1 = H_2/a$
Frequency	$f_1 = f_2/a$
Wavelength	$\lambda_1 = a\lambda_2$

1.2 Allowed and forbidden processes

Similarity laws are not necessarily obeyed; they are obeyed only when a certain set of elementary processes, which are termed allowed, occur in the discharge. The processes for which the similarity laws are violated are called forbidden. The violation of a similarity law signifies that some forbidden processes play an important role in the discharge.

In completely similar discharges, the rate of charged-particle production $\mathrm{d}n/\mathrm{d}t$ in the gap volume is expressed in terms of the constant a as

$$\left(\frac{\mathrm{d}n}{\mathrm{d}t}\right)_1 = a^{-3}\left(\frac{\mathrm{d}n}{\mathrm{d}t}\right)_2 . \qquad (1)$$

Consequently, for a volume elementary process to be allowed, relation (1) must be satisfied. By the following examples, we show which processes satisfy this relation and which do not, i.e., we give examples of allowed and forbidden processes.

Ionization at single collisions. For equal electron energies, the ionization rate $\mathrm{d}n/\mathrm{d}t$ is proportional to the electron density and the neutral particle density n_0:

$$\left(\frac{\mathrm{d}n}{\mathrm{d}t}\right)_1 = cn_1n_{01} = c\,\frac{n_2}{a^2}\,\frac{n_{02}}{a} = a^{-3}\left(\frac{\mathrm{d}n}{\mathrm{d}t}\right)_2 . \qquad (2)$$

Hence, the process under consideration is allowed.

Electron attachment and detachment. The attachment rate, like the ionization rate at single collisions, is proportional to the density of electrically negative particles and the electron density. The attachment is therefore an allowed process. When the detachment occurs in negative ion – molecule collisions, this process is also allowed.

Drift and diffusion. The rate of charged-particle production or loss at a given point due to the drift motion is determined in terms of the flux as $\mathrm{d}n/\mathrm{d}t = \mathrm{d}(nv)/\mathrm{d}x$, where v is the drift velocity. Hence, we obtain $(\mathrm{d}n/\mathrm{d}t)_1 = a^{-3}(\mathrm{d}n/\mathrm{d}t)_2$, i.e., the electron drift is allowed. From the diffusion equation $\mathrm{d}n/\mathrm{d}t = -D(\mathrm{d}^2n/\mathrm{d}x^2) \sim \lambda v_1(\mathrm{d}^2n/\mathrm{d}x^2)$, where D is the diffusion coefficient proportional to the mean free path λ and the random electron velocity v_1, it is easy to conclude that diffusion is also an allowed process.

Secondary processes at the electrodes. Apart from the processes occurring in the gap volume, of great importance are secondary processes at the electrodes. The electron current densities due to the secondary processes should be related as $1/a^2$. This allows showing that among the allowed secondary processes are the secondary electron emission due to ion and atom bombardment and photoemission from the cathode.

Charge exchange. In the charge exchange, fast ions exchange charges with neutral molecules in collisions with them and in doing so do not lose their kinetic energy. Such a collision gives rise to a slow ion and a fast neutral molecule. The rate of production of such molecules is proportional to the densities of the ions and gas molecules, i.e., to n_+n, and is therefore transformed with the factor $1/a^3$. Therefore, this process is allowed.

Recombination. The recombination between positive and negative particles obeys the law

$$\frac{\mathrm{d}n}{\mathrm{d}t} = -\beta n_+ n_- , \tag{3}$$

where β is the recombination rate coefficient. For high gas pressures, $\beta \sim 1/p$ and therefore this coefficient transforms with the factor a, while each of n_+ and n transform with the factor $1/a^2$, and therefore $\mathrm{d}n/\mathrm{d}t$ scales with the factor $1/a^3$ and the process is allowed. For a low gas pressure, recombination is a forbidden process because $\beta \sim p^{1/2}$ or $\beta = \text{const}$.

The Penning effect. When an excited molecule of one gas collides with a neutral molecule of another gas and ionizes it, this is an allowed process. This process, which may occur when the ionization potential of one gas exceeds the ionization potential of the other, is a kind of stepwise ionization. Also among the allowed processes is secondary emission from the electrodes caused by ions, electrons, nonresonance photons, and metastable atoms, as well as fast neutral particles.

Among the forbidden processes are all types of stepwise ionization, collisions of the second kind except the Penning effect, gas photoionization, the charge exchange between a fast neutral particle and an ion, all kinds of recombination (except for the recombination occurring for a high gas pressure as discussed in Section 1.1), the thermal ionization of gas, the photoeffect produced by diffusing resonance photons, and thermoionic and field emission, as well as explosive electron emission and the desorption of charged or neutral particles.

Extreme caution must be exercised in resorting to similarity laws. When these laws are obeyed, all forbidden processes may be thought of as being eliminated. However, it is invalid to assume that forbidden processes are necessarily present when these laws are violated. If a discharge first obeys the similarity laws and then departs from them when some parameter, e.g., the current, changes, it is difficult to understand what underlies the departure: the occurrence of forbidden processes or a variation in the gas temperature.

We now address the notions of discharge and breakdown. In the literature, these terms are sometimes considered synonyms, but they are in fact different. A discharge comprises three stages: a breakdown, a spark, and an arc. However, in this review, as in other papers, we use these words as synonyms.

2. Similarity laws for static and microwave discharges

2.1 The Townsend mechanism

Any discharge commences with the emergence of free electrons in the discharge gap. Those electrons that are close to the cathode are highest in efficiency. We consider a gas discharge between plane electrodes across which an electric voltage is applied. The primary electron ionizes the atoms and molecules of the gas. The number of new electrons produced in transit through a 1 cm path is termed the collisional ionization coefficient and is denoted by α. The current flowing through the discharge gap is then given by

$$i = i_0 \exp(\alpha d) , \tag{4}$$

where d is the gap length and i_0 is the initial electron current from the cathode. Sometimes, in lieu of the coefficient α, use is made of the coefficient η given by the number of new electrons produced by the primary electron in its passage through a potential difference of 1 V or of the ionizing collision frequency ν given by the number of collisions per 1 s. Clearly,

$$\eta = \frac{\alpha}{E} , \tag{5}$$

$$\nu = \frac{\alpha}{v} , \tag{6}$$

where v is the electron drift velocity.

Apart from gas ionization with the production of new electrons and ions, inelastic collisions also occur, with the resultant production of excited molecules followed by the emission of photons or the production of molecules in metastable states. Subsequently, ions, photons, and metastable atoms produce secondary electron emission from the cathode. Moreover, gas photoionization may occur under certain conditions.

We consider the classical case of a non-self-sustained discharge, where the secondary electrons are produced due to positive-ion bombardment of the cathode [1–5]. Let i be the electron current arriving at the anode, i_0 be the initial electron current emanating from the cathode under external influence, e.g., under ultraviolet irradiation, i_+ be the electron current emanating from the cathode due to positive-ion bombardment, and γ be the number of electrons ejected from the cathode per one incident positive ion. Then

$$i = (i_0 + i_+) \exp(\alpha d) , \tag{7}$$

$$i_+ = \gamma \left[i - (i_0 + i_+) \right] . \tag{8}$$

By eliminating i_+ from system of equations (7) and (8), we obtain

$$i = i_0 \frac{\exp(\alpha d)}{1 - \gamma \left(\exp(\alpha d) - 1 \right)} . \tag{9}$$

The coefficient γ obeys the similarity law $\gamma = f(E/p)$. A more general meaning may be assigned to this coefficient if it is assumed that γ denotes the number of secondary electrons from the cathode per one electron produced by collisional ionization. Under this assumption, the coefficient γ characterizes the electron yield from the cathode due to ions and photons.

The quantity $\gamma \left(\exp(\alpha d) - 1 \right)$ is very small for weak electric fields E but increases with the field up to the value

$$\mu = \gamma \left(\exp(\alpha d) - 1 \right) = 1 . \tag{10}$$

In this case, the denominator in expression (9) vanishes and the current i becomes infinitely large. Condition (10) signifies that every primary electron that drifts from the cathode produces one secondary electron due to secondary processes. Because $\exp(\alpha d) \gg 1$, condition (10) is simplified to $\gamma \exp(\alpha d) = 1$. Formula (10) is the Townsend breakdown criterion for a gas gap. However, using this criterion for deriving the similarity law in a static discharge requires considering the dependence of α on the field strength E and the gas pressure p in greater detail.

According to Townsend, the character of the dependence of α on the electric field strength E may be determined from the following simple argument. Let the energy gained by an electron over its mean free path be equal to $Ee\lambda$. If $Ee\lambda \geqslant eU_i$, where U_i is the gas ionization potential, the electron ionizes the gas. The number of collisional ionization events over a unit path length is then equal to the total number of electrons that begin to move times the probability that the mean free path $\lambda > \lambda_i = U_i/E$. According to the kinetic theory, the fraction of electrons N/N_0 whose free path exceeds some fixed value λ_i is

$$\frac{N}{N_0} = \exp\left(-\frac{\lambda_i}{\lambda_0}\right) = \exp\left(-\frac{U_i}{\lambda_0 E}\right), \tag{11}$$

where λ_0 is the mean free path. With (11), we obtain

$$\alpha = \frac{1}{\lambda_0}\exp\left(-\frac{U_i}{\lambda_0 E}\right), \tag{12}$$

and because the mean free path is inversely proportional to the gas pressure, formula (12) can be rewritten as

$$\frac{\alpha}{p} = A\exp\left(-\frac{AU_i p}{E}\right) = A\exp\left(-\frac{Bp}{E}\right). \tag{13}$$

Experiments confirm that in a certain range of E/p values, the dependence is of precisely this type. But the constant coefficients A and B differ from the coefficients calculated under crude approximations. In practice, use is made of experimental $\alpha/p = f(E/p)$ curves or of approximations of type (13) with A and B selected from the best fit to measurement data. Quite frequently, other approximations that allow simplifying mathematical calculations are used. This issue is discussed in greater detail in Section 2.2.

2.2 The Paschen law

The Townsend gas breakdown theory permits explaining the experimentally observed dependence known as the Paschen law, which consists of the following. When the discharge gap length d and the gas pressure p are varied in such a way that their product remains constant, the static breakdown voltage also remains constant. To derive the Paschen law in analytic form, we use the Townsend self-sustained discharge condition (10) and formula (13) for $\alpha/p = f(E/p)$. Hence, we obtain

$$pd\,\frac{\alpha}{p} = \ln\left(1+\frac{1}{\gamma}\right). \tag{14}$$

Upon substitution of α/p from expression (13), we obtain

$$U_s = \frac{Bpd}{\ln\left[Apd/\ln(1+1/\gamma)\right]} \tag{15}$$

for the static breakdown voltage. The function $U_s(pd)$ has a minimum

$$U_s^{\min} = B(pd)_{\min}, \tag{16}$$

where

$$(pd)_{\min} = \frac{\exp(1)}{A}\ln\left(1+\frac{1}{\gamma}\right). \tag{17}$$

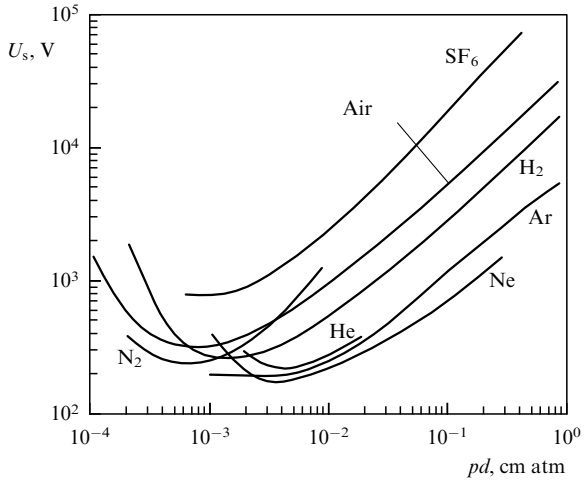

Figure 1. Breakdown voltage versus the product pd for different gases (Paschen curves).

Typical Paschen curves for several gases obtained by generalizing the data from many papers are plotted in Fig. 1 [3]. For every gas, the breakdown voltage decreases with decreasing pd to attain a minimum for some value $(pd)_{\min}$, and then increases. Impurities in gases, as well as the cathode material, may exert an effect on the magnitude of the breakdown voltage because the α and γ coefficients vary in this case. We note that the γ coefficient is not necessarily a function of E/p, but it is nevertheless difficult to reveal departures from the Paschen law because γ is involved the double logarithm. In the breakdown of air, γ varies from 10^{-4} (for relatively low pressures) to 10^{-8} (at atmospheric pressure). In this case, $\ln\ln(1/\gamma)$ changes by only 30%. This is the reason why the theory under discussion was long considered to apply to the breakdown for both low and high pressures, because it yielded approximately correct values of the breakdown voltages.

But it was discovered more recently that the breakdown voltage is independent of the cathode material at pressures around the atmospheric pressure. At present, the self-sustained breakdown criterion in the form of Eqn (10) is believed to apply only to gas breakdown at decreased pressure. Also, it should be noted that Eqn (10) is a simplification. The issue of current buildup in gas breakdown is more complicated. It is considered at length in monograph [5]. In particular, electrons may be knocked out of the cathode not only by ions but also by photons and the excited atoms and molecules of gas in the resonance and metastable states that diffuse to the cathode [6].

In some cases, departures from the Paschen law occur. First, departures are observed for strong electric fields in the gap, which takes place primarily in the right-hand side of the Paschen curve at high gas pressures, as well as in the breakdown of electrically strong gases, e.g., sulfur hexafluoride. Second, the Paschen law is violated in the far left part of the pd range, where the conditions in the gap approach vacuum conditions. Third, the Paschen law is sometimes violated for short gaps in the neighborhood of the minimum of $U_s(pd)$. As shown in Ref. [3], these departures are attributable to the occurrence of field and explosive electron emissions, which are forbidden processes as noted in Section 1.2. Strong departures from the Paschen curve, which depend on the distance d, are observed in the right-

Table 2.

Gas	E/p, V (cm Torr)$^{-1}$	A, (cm Torr)$^{-1}$	B, V (cm Torr)$^{-1}$
Nitrogen	27 – 200 100 – 600	8.8 12	275 342
Air	36 –180 100 – 800	8.6 15	254 365
Hydrogen	22 – 1000	5	139
Oxygen	70 – 300	7.7	203.5
Carbon dioxide	44 – 150 500 – 1000	4.75 20	182.5 466
Methane	40 – 125	7	192.1
Acetone	74 – 400	14.3	360.8
Benzene	160 – 650	26	601.3
Helium	3 – 10 20 – 150	3 3	25 34
Neon	100 – 400	4	100
Argon	100 – 600	12	180
Krypton	100 – 1000	17	240
Xenon	200 – 800	26	350
Mercury	200 – 600	20	370

hand side of the dependence $U_s(pd)$ for sulfur hexafluoride [7].

Apart from these so-called electrofield departures from the similarity law, other departures are also observed. For instance, measurements in hydrogen for an interelectrode distance $d = 0.4-3$ cm in the voltage range up to 30 kV showed that U_s is a function of $pd^{0.5}$ rather than pd [8]. For $pd \approx 1.5$ cm Torr in helium, the breakdown voltage is not uniquely determinable [9]. For $pd \ll (pd)_{\min}$, a specific form of discharge may exist, which is referred to as a high-voltage glow discharge, in which the ignition voltage is equal to the discharge operating voltage [10, 11].

We now briefly reconsider the dependence of α/p on E/p. According to the simplest Townsend theory, this dependence is defined by formula (13). It is quite frequently used as an empirical dependence in the analytic representation of the experimental data on α measurements. The coefficients A and B for different gases and E/p values are collected in Table 2 [12]. The experimental dependence of α/p on E/p for air in the range $40 < E/p < 140$ V cm^{-1} Torr^{-1} is approximated by the Sanders formula [13]

$$\frac{\alpha}{p} = A_0\left[\frac{E}{p} - B_0\right]^2, \tag{18}$$

where $A_0 = 1.17\times10^{-4}$ cm Torr V^{-2}, $B_0 = 32.2$ V cm^{-1} Torr^{-1}. In what follows, we use this formula to verify the validity of the similarity law for pulsed discharges.

It is worth noting that the effect of electron attachment, which is characterized by the coefficient η, is not included in the above formulas for air. Because this coefficient usually occurs in formulas as $(\alpha - \eta)$, it is implied that in all cases it is included in the effective collisional ionization coefficient $\alpha_{\text{eff}} = \alpha - \eta$.

2.3 Similarity laws for microwave discharges

Discharges in which the wavelength λ of the applied electric field is comparable to the cathode – anode distance d are said to be microwave discharges. Characteristic of a microwave range is a small electron oscillation amplitude in comparison with the dimensions of the discharge volume. There are continuous and pulsed microwave discharges. In this section, we consider continuous discharges, while pulsed ones are discussed in Section 6. The similarity laws are equally applicable to microwave discharges. For similarity parameters, use is commonly made of combinations such as $p\lambda$, $E\lambda$, $E\Lambda$, E/p, $p\Lambda$, and Λ/λ, where Λ is called the diffusion length. For plane parallel electrodes, it is typically assumed that $\Lambda \approx d/\pi$ [14].

The approach developed by Townsend for constant electric fields, which we considered in Section 2.1, was found to be beneficial for the description of a microwave discharge. In classical static discharges, new electrons are produced due to the secondary electron emission and the ionization of gas, and vanish on arrival at the anode. In microwave discharges, electrons are produced by ionization of the atoms and molecules of gas and disappear primarily due to diffusion. We do not take the electron attachment and recombination into account. If the electron production rate is equal to the loss rate, a stationary state sets in. But if the electron production rate is greater, even if only slightly greater than the loss rate, the electron density rises steeply with the onset of a breakdown.

We now determine how the diffusion rate enters the equation that describes the increase in the electron density. For this, we write the approximate equation for the ionization rate as [4, 14]

$$\frac{\mathrm{d}n}{\mathrm{d}t} = \left(\nu - \frac{D}{\Lambda^2}\right)n, \tag{19}$$

where D/Λ^2 is the diffusion rate, D is the diffusion coefficient, ν is the ionization frequency, and n is the electron plasma density. The density variation rate is proportional to the density and the difference between the electron production rate due to ionization and the loss rate due to diffusion. Although ν and D/Λ^2 are typically not constants, to estimate the order of magnitude, we assume that they are independent of our variables. We integrate Eqn (19) to obtain

$$n = n_0 \exp\left[\left(\nu - \frac{D}{\Lambda^2}\right)t\right]. \tag{20}$$

Each of the terms appearing in the exponent is so large that the electron density builds up rapidly even when ν is only slightly higher than D/Λ^2, thereby confirming the Townsend criterion, which is taken as the equality between the ionization and loss rates, i.e.,

$$\nu = \frac{D}{\Lambda^2}. \tag{21}$$

When microwave frequencies are used, the electric field oscillates fast, such that an electron does not manage to move far away from its initial position during the period of the force it experiences. This implies that the electron does not escape from the discharge region, as is usually the case with lower-frequency operation. The electrons leave the discharge region only by way of diffusion and may be lost inside the discharge region itself due to recombination and electron attachment.

Only a relatively small number of electrons with a high energy collide with the vessel walls. That is why there is no need to consider the production of secondary electrons at the walls; all electrons are produced by ionization inside the discharge gap.

We consider this process in greater detail; for this, we consider the motion of an individual electron whose initial energy is assumed to be zero. The electric field accelerates the electron during a short time interval until either the field changes its sign or the electron collides with an atom. The collision, generally speaking, changes the direction of electron motion, but the loss of speed is insignificant. The atom is imparted only a part of the energy, equal to $2m/M$ on average, where m and M are the respective masses of the electron and the atom. Upon collision, the electron is once again accelerated by the electric field during the next short time interval. The electron energy increases and decreases in small portions, the energy gain depending on the applied electric field strength and, generally speaking, exceeding the energy decrease.

When the kinetic electron energy attains a value exceeding the lower atomic excitation potential, there is a finite probability for the next collision to be inelastic. Such a collision then results in the internal energy of the atom being changed and the electron losing the major part of its energy. When the thus excited atomic state is not metastable, the atom practically instantly returns to the initial state upon emitting the characteristic radiation. When the electric field is strong enough, some electrons acquire an energy that exceeds the ionization energy without experiencing an inelastic collision. In this case, a collision may give rise to a secondary electron and a positive ion. In a sufficiently strong field, such collisions occur so frequently that the electron production rate exceeds the loss rate, with the consequential onset of breakdown. With the diffusion coefficient $D = \lambda_0 v/3 = v^2/3\nu$, where v is the electron drift velocity, criterion (21) becomes

$$\frac{\alpha}{p} = \frac{1}{\sqrt{3}p\Lambda}\,. \tag{22}$$

This is the microwave breakdown criterion, whence it follows that the quantity E/p is a single-valued function of $p\Lambda$, because α/p depends only on E/p. Dependence (22) therefore obeys the similarity law. But for similarity parameters in the case of a microwave breakdown, the combinations $E\lambda$ and $p\lambda$ are typically used. In this case, for a given wavelength λ of the microwave voltage, it is possible to determine the simple dependences of E on p. Shown in Fig. 2, for instance, are the E-versus-p curves for the continuous-regime breakdown in air, oxygen, and nitrogen.

As regards physical processes, an optical gas breakdown is similar to the microwave breakdown. Breakdown of a gas at optical frequencies requires fields of $10^6 - 10^7$ V cm^{-1} in the light wave. For this, focused ruby-, neodymium-, or CO_2-laser beams are commonly used. The dependences $E(p)$ for the optical breakdown also have a minimum, as in the cases of a constant field or a microwave field. However, as is evident from Fig. 3, this minimum is in the pressure range $10^2 - 10^3$ atm [15]. For nitrogen, for instance, $p_{\min} \approx 10$ Torr for the frequency 9.4×10^9 Hz; for the ruby laser frequency 4.3×10^{14} Hz, $p_{\min} \approx 10^5$ Torr, i.e., four orders of magnitude higher. The ruby laser frequency is higher by equally many orders of magnitude. This is consistent with the similarity law

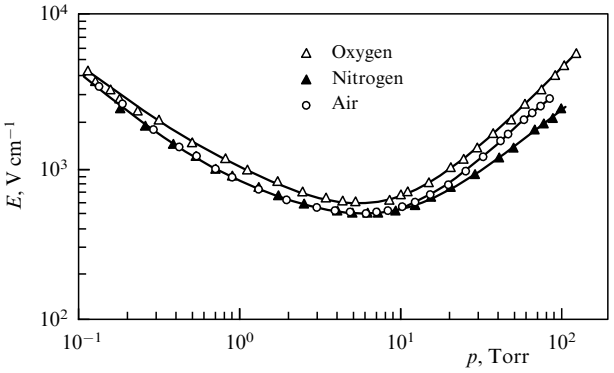

Figure 2. Continuous-mode breakdown in air, oxygen, and nitrogen at the frequency 9.4 GHz for $\Lambda = 0.4$ cm.

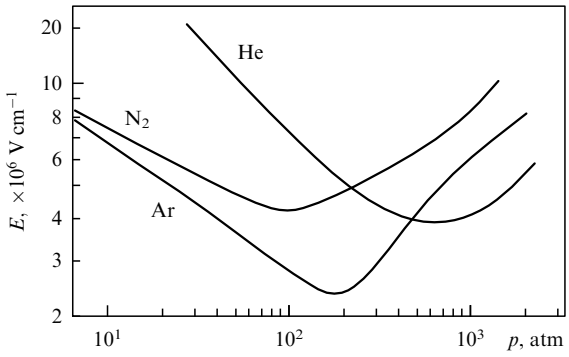

Figure 3. Thresholds for the Ar, N_2, and He breakdown by a ruby laser in a wide pressure range. The pulse duration is 50 ns, the at-focus diameter is 0.1 mm.

because $(p\lambda)_1 = (p\lambda)_2$ or $(p/f)_1 = (p/f)_2$, where f is the alternating field frequency. We emphasize that the optical breakdown normally occurs for a pulsed voltage with the duration $t_i = 10^{-9} - 10^{-8}$ s. But the oscillation period of laser radiation $T \ll t_i$, and therefore this discharge should be placed among stationary discharges.

3. Similarity law for the time of pulsed discharge formation

3.1 Breakdown delay time

In the first experiments to investigate the pulsed breakdown of a gas gap [16], it was already shown that the instant at which the static breakdown voltage U_s is reached and the instant of gap breakdown are separated in time by some interval t_d, which is termed the breakdown delay. Generally, the number of breakdowns n_t with a time delay t or longer depends on the time delay as

$$n_t = n_0 \exp\left(-\frac{t+\tau}{\sigma_0}\right), \tag{23}$$

where σ_0 is the statistically averaged delay time, n_0 is the total number of breakdowns, and τ the shortest time for the breakdown delay time under given conditions. The time delay t_d is the sum of the statistical time delay σ and the discharge formation time, which is the quantity τ in formula (23), i.e.,

$$t_d = \sigma + \tau\,. \tag{24}$$

The value of σ is determined by the electron current i_0 from the cathode and is statistical in character. The dependence of i_0 on σ_0 has the form [16]

$$i_0 = \frac{e}{\sigma_0} w_1 w_2 , \tag{25}$$

where e is the electron charge, w_1 is the probability that an initiating electron emerges from the cathode in the domain where it may lead to a breakdown, and w_2 is the probability that this electron leads to the breakdown. The value of σ_0 is determined from the slope of the straight line $|\ln(n_t/n_0)| = (t+\tau)/\sigma_0$. For gaps with a length of the order of several millimeters, in the absence of external irradiation sources and a voltage nearly twice as high as the static breakdown (Paschen) voltage, $w = w_1 w_2 \approx 1$ [16]. Consequently, the electron current from the cathode is then given by

$$i_0 = \frac{e}{\sigma_0} . \tag{26}$$

This formula is widely used in measurements of the electron current emitted from the cathode on application of a pulsed voltage across the gap. The magnitude of this current allows estimating the cathode surface finish. It follows from (26) that σ_0 is nothing but the mean time interval between the emergence of two initiating electrons. There is a limiting value of the current i_0 above which it cannot be measured from the slope of the straight line $|\ln(n_t/n_0)| = (t+\tau)/\sigma_0$. This is the case for $\sigma_0 < \tau$.

To measure the discharge formation time τ, it is normally desirable to make $\sigma_0 \ll \tau$. Only in this case is it possible to accurately measure this quantity and use it to judge the discharge mechanism. To shorten σ_0, ultraviolet radiation sources are used to illuminate the cathode surface and increase i_0. As a rule, these are mercury lamps or spark sources. It should be borne in mind that the total intensity of external radiation (for instance, of cosmic rays) is usually negligible: about 10 electrons per s per cm^3 of the air volume. When there are no special auxiliary electron sources, the discharge is initiated due to the electrons emitted by the cathode itself. Among the mechanisms responsible for this are the following [3].

1. Electron emission caused by dielectric films and cathode surface inclusions due to the Malter effect (the anomalous emission through dielectric films on the cathode) and due to the Paetow effect (the field emission enhanced by the charging of dielectric films and inclusions on the cathode surface).

2. Exoelectron emission. For electrodes fabricated without special processing, the exoelectron current from the cathode normally does not exceed 100–1000 electrons per cm^2 per s. This current may influence the breakdown caused only by millisecond pulses.

3. Field emission. For an average field $E_0 = 10^5 - 10^6$ V cm^{-1}, this kind of emission plays the main role in the delivery of initiating electrons. To obtain a field-emission current of 10^{-10} A, whereby the statistical delay time is around 10^{-9} s, a tungsten cathode surface of 1 cm^2 requires the electric field strength about 2×10^7 V cm^{-1}. Our concern is with a pulsed electric gas discharge for the field strength $10^5 - 10^6$ V cm^{-1}.

Numerous investigations of the prebreakdown conduction in a vacuum gap for $E = 10^5 - 10^6$ V cm^{-1} reveal the occurrence of the electron current $10^{-5} - 10^{-3}$ A and show that the dependence of this current on the average field strength in the gap is in qualitative agreement with the Fowler–Nordheim formula for the field emission. This is attributable to the existence of micropoints on the electrode surface, which have a field strength E_0 far greater than the average field $E = U/d$. The quantity E_0/E is termed the electric field enhancement factor.

3.2 Townsend breakdown

As is well known, a gas-discharge gap is not broken down for some time when a pulsed voltage U exceeds the static breakdown voltage U_s, i.e., the Paschen one. The quantity

$$\delta = \frac{U - U_s}{U_s} , \tag{27}$$

which is termed the overvoltage, determines the mechanism of a gas discharge. For small δ, the Townsend mechanism occurs, whereby each electron that starts from the cathode gives rise to an electron avalanche due to collisional ionization of atoms or molecules in the gas, as discussed in Section 2.1. The number of electrons in such an avalanche grows exponentially, $N = \exp(\alpha x)$. Apart from the number of electrons, the number of ions and excited atoms or molecules of the gas grow in accordance with the same exponential law. They are deexcited with the emission of photons. When arriving at the cathode, ions and photons give rise to the emission of secondary electrons. The number of secondary electrons μ is determined from formula (10). In the static breakdown, $\mu = 1$ and, as shown in Section 2.1, we obtain the Paschen law. For a pulsed breakdown, $\mu > 1$. A distinguishing feature of the Townsend mechanism is that the space charge of the primary isolated avalanche does not distort the electric field in the gap, and the number of electrons in the avalanche is always less than some critical N_c,

$$\exp(\alpha d) < N_c . \tag{28}$$

When the number of electrons and ions in the avalanche reaches N_c, the field of the space charge becomes comparable to the external field E_0 and the discharge mechanism changes from the Townsend to the streamer one. Because the overvoltage coefficient increases with E, its magnitude plays the decisive role in passing from the Townsend discharge mechanism to the streamer one. Figure 4 shows the curve dividing the values of pd and of the overvoltage coefficient δ in the air discharge into two domains [17]. When the discharge conditions correspond to the domain above the curve, the

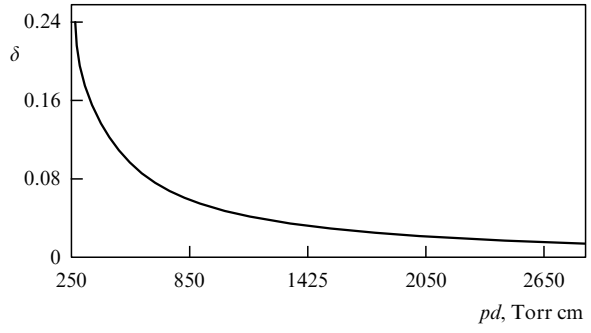

Figure 4. The curve that separates the domains of air discharge development according to the Townsend and streamer (above the curve) mechanisms.

streamer discharge mechanism occurs; the Townsend mechanism occurs in the lower domain. Hence, the Townsend discharge at atmospheric and higher pressures for $d = 1$ cm occurs only for $\delta < 0.1$. For higher overvoltages, a streamer discharge occurs.

The breakdown formation time τ for a pulsed Townsend breakdown was determined by Schade [18, 5]. Let i_0 be the initial current from the cathode; $i(t)$ be the total electron current from the cathode at an instant t; $i_a(t)$ be the total electron current at the anode at t; $i_+(t)$ be the positive-ion current at the cathode at t; $i_{a+}(t)$ be the ion current at the anode at t; and τ_+ be the anode-to-cathode ion traveling time. Then, assuming that the principal secondary process is the ion-driven ejection of electrons from the cathode, we can write the relations

$$i = i_0 + \gamma i_+ , \tag{29}$$

$$i_+ = i_{a+}(t - \tau_+) , \tag{30}$$

$$i_{a+} = i_a - i , \tag{31}$$

$$i_a = i \exp(\alpha d) , \tag{32}$$

whence it follows that

$$i(t) = i_0 + \gamma \left(\exp(\alpha d) - 1\right) \left[i(t) - \tau_+ \frac{\mathrm{d}i(t)}{\mathrm{d}t} \right] . \tag{33}$$

We introduce the notation $\gamma (\exp(\alpha d) - 1) = \mu$, integrate Eqn (33), and assume that the discharge formation time τ is reached for $i/i_0 = \text{const}$ to obtain

$$\tau = \frac{\mu \tau_+}{\mu - 1} \ln \frac{1 + (\mu - 1)(i/i_0)}{\mu} . \tag{34}$$

Because α strongly depends on the field strength, the time τ shortens rapidly with increasing the overvoltage. Indeed, for a small increase in the field strength from E_s, to $E = E_s + \Delta E$, we have $\alpha = \alpha_s + \Delta\alpha$, from with an increment $\Delta\alpha$. We use formula (13) for α to obtain [5]

$$\Delta\alpha = \frac{ABp^2 \Delta E}{E_s^2} \exp\left(-\frac{Bp}{E}\right) , \tag{35}$$

where E_s is the statistical electric breakdown strength. We then have

$$\mu = \gamma \left\{ \exp\left[(\alpha_s + \Delta\alpha)\, d\right] - 1 \right\} \approx 1 + d\Delta\alpha , \tag{36}$$

because it is assumed that $\gamma [\exp(\alpha_s d) - 1] = 1$ and $\gamma \ll 1$. The quantity α_s is the magnitude of the collisional ionization coefficient in the static gap breakdown. By substituting expressions (35) and (36) in formula (34), we obtain the time τ as

$$\tau = \frac{E_s^2 \tau_+}{ABp^2 \Delta E d} \exp\left(\frac{Bp}{E}\right) \times \ln\left[1 + \frac{ABp^2 \Delta E\, d}{E_s^2} \exp\left(-\frac{Bp}{E}\right) \frac{i}{i_0}\right] . \tag{37}$$

Because $i/i_0 \gg 1$ in the breakdown, the logarithmic term can be considered constant, to be denoted as $\ln \Gamma$ in what follows. Relation (37) implies that

$$p\tau = \frac{(E_s/p)^2 \exp(Bp/E)}{ABv_+(E/p)(E_s/p - E/p)} \ln \Gamma , \tag{38}$$

where v_+ is the ion drift velocity. It is easily seen that

$$\frac{E/p - E_s/p}{E_s/p} = \frac{U - U_s}{U_s} = \delta ,$$

which is the overvoltage. If it is assumed that $v_+ \approx cE_s/p$, then it follows from formula (38) that

$$p\tau = \frac{\exp(Bp/E)}{ABc\delta} \ln \Gamma . \tag{39}$$

Because the values of the voltages U_s and E_s/p in the static breakdown are functions of pd, in accordance with the Paschen law, it follows from formula (39) that the similarity law applies to the Townsend pulsed discharge. In this case, the value of $p\tau$ depends on two combinations, E/p and pd. The experimental data in Refs [16, 19] for decreased gas pressures confirm the validity of formula (38) for air for centimeter-long gaps $pd < 200$ Torr.

Above this limit, however, the time τ is many times shorter than the value that follows from formula (37). Many authors have endeavored to resolve these contradictions. These works are outlined in monographs [16, 19]. The streamer discharge mechanism was developed on their basis.

3.3 The streamer discharge mechanism

When the number of charged particles (electrons and ions) in an avalanche reaches some value N_c, a streamer discharge sets in. The space charge of the avalanche consists of an electron cloud in its head and an ion cloud in its tail (Fig. 5). Due to this charge, the electric field is enhanced in front of and behind the avalanche and weakened inside it. Furthermore, conditions for the emergence of secondary electrons in the enhanced-field regions occur in the gas due to the photoionization of easily ionizable gas impurities [20, 21] and the extrusion of electrons at the front of the avalanche head by Coulomb forces [22] or runaway electrons due to the high

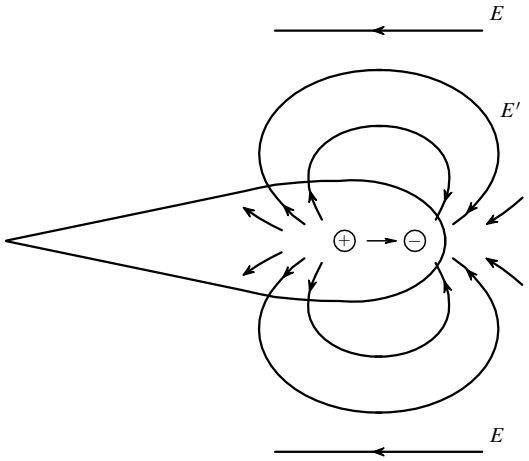

Figure 5. Schematic drawing of an individual avalanche and the field lines: E is the external field and E' is the space charge field of the avalanche electrons and ions. The centers of opposite space charges are conventionally shown by circles.

total electric field in the avalanche head [24]. The secondary electrons produce new avalanches, whose ion component is drawn into the electron head of the primary avalanche to produce a conducting plasma — a streamer with a velocity several orders of magnitude higher than the electron drift velocity v. If the number N_c of electrons is attained in the avalanche over the path traveled by the avalanche, $x_c < d$, then the streamer is directed from the cathode to the anode. It is then called the anode-directed streamer. But if $x_c \simeq d$, then an a cathod-directed streamer is formed. The speed with which the streamer propagates is much larger than the speed v of the electron drift.

If it is assumed that the discharge was formed after the streamer bridged the anode–cathode gap, the following relation applies to the streamer discharge formation time:

$$\tau = \frac{\ln N_c}{\alpha v} . \tag{40}$$

If N_c is independent of E, d, and p, it follows from formula (40) that the streamer discharge mechanism obeys the similarity law $p\tau = F(E/p)$.

Proceeding from the experimental data on electron avalanches in a Wilson chamber, Raether [25, 26] arrived at the following conclusion: in gaps with a length of the order of 1 cm, the streamer discharge mechanism operates and the discharge formation time τ is determined by the time an avalanche, even if caused by one electron, takes to grow to dimensions for which the avalanche transforms into a streamer. The streamer develops much faster than the avalanche, and its buildup time may be neglected. It was assumed that the avalanche turns into a streamer in air when the number of electrons in the avalanche is exp20, i.e., when $\alpha x = 20$, where α is the collisional ionization coefficient and x is the path length over which the avalanche accumulates the required number of electrons. Because $x = vt$, we have

$$p\tau = \frac{20}{v\,(\alpha/p)} . \tag{41}$$

Experimental data were shown to be in good agreement with formula (41) for air and other gaps with a length of the order of several centimeters [19]. In the discharges discussed below, the pressure is about 1 atm or higher, and the electric field strength amounts to 10^5 V cm^{-1} and above. Under these conditions, the electron avalanche development time is 10^{-9} s or shorter. This brings up the question of how much similarity law is violated under these conditions. The situation is facilitated by the fact that the main parameters that determine the electron avalanche development, α/p, v, and the electron energy ε, depend only on the ratio E/p and not on E and p separately [16].

To calculate the time τ, it is vital to know the electron drift velocity. Summarized data for high E/p show that

$$v = c\left(\frac{E}{p}\right)^{\varkappa} . \tag{42}$$

The corresponding data for c and $\varkappa$ for several gases are collected in Table 3 [12].

Among the points at issue is the statement that the electric field has no effect on the value of N_c for gaps $d \geqslant 1$ cm. Several attempts have been made to take this effect into account. For instance, Fletcher [27] solved the equations describing the development of an electron avalanche with the inclusion of diffusion electron expansion, as well as the spatial electron and ion charge distribution in an atmospheric air discharge. But he eventually arrived at the conclusion that the available experimental data for fields below 10^5 V cm^{-1} agree well with the theory if it is assumed that $N_c = 10^8$, independently of E. This is attributable to the fact that the time τ depends only slightly on N_c, because the latter occurs in the logarithm. Consequently, the numerator in formula (41) should be 18.4 and not 20. This difference is normally within the experimental error.

Table 3.

Gas	E/p, V (cm Torr)$^{-1}$	c	$\varkappa$
N_2	120 – 3000	3.3×10^6	0.5
	300 – 4000	—	—
O_2	100 – 8000	3.75×10^6	0.5
	200 – 2000	—	—
CO_2	150 – 2000	1.58×10^6	0.59
	5000 – 5000	—	—
	45 – 220	—	—
CH_4	120 – 1000	5.80×10^5	0.76
	300 – 5000	—	—
	50 – 200	—	—
Air	130 – 300	3.3×10^6	0.5
	10 – 130	3.3×10^5	1

However, this issue invites further consideration, because the question of whether N_c depends on E and p is central to the statement that the breakdown formation time obeys the similarity law in the streamer discharge mechanism. Simple estimates show that the external electric field is severely distorted by the avalanche space charge when $N = N_c$ [26], and for definiteness it is commonly assumed that the change-over condition is that the field inside the avalanche is equal to the external field, i.e., that the total field vanishes inside the avalanche. However, this condition makes no mention of the possibility that secondary electrons emerge in front of the propagating streamer. Most often considered as a mechanism that provides the secondary electrons is photoionization, with the implicit assumption that its intensity is high enough when $N \approx N_c$.

It is pertinent to note that although this criterion is empirical, it was introduced not on the basis of measurements of the number of electrons in the avalanche or, even more so, of the fields inside the avalanche and its head, but starting from the experimental fact that the initial speed of avalanche head propagation is equal to the electron drift velocity and then increases steeply. Experimentally, it is easiest to measure either x_c or t_c and then calculate N_c. It is easily seen that N_c is only crudely estimated owing to the exponential dependence of N on αvt.

Therefore, although the avalanche-to-streamer change-over is objectively observed in experiments, the quantitative criterion $N = N_c$ reflects nothing more than the idea of an external field distortion by the space charge. That is why a detailed consideration of the physical processes that accompany the avalanche-to-streamer change-over is significant. Special emphasis is placed on matters such as the description of the spatial structure of electron and ion clouds, the description of the spatial field distribution at different time instants, and the elucidation of the physical mechanisms responsible for the secondary processes.

As shown in Ref. [23], the diffusion broadening of an electron cloud in the avalanche proceeds until the number of electrons in it reaches a value $N \sim 10^6$ (for N_2, O_2, CH_4). Then, on exceeding this value, electrostatic electron repulsion sets in, the electrons in the avalanche head having a speed higher than v. The growth in the number of electrons in the avalanche then begins to depart from the exponential growth and moderates. This effect, referred to as avalanche self-breaking [23], is interpreted by the theory [12] and is recorded experimentally [26], but has no effect of any significance on the applicability of the similarity law for the time τ. (These issues are discussed in greater detail in Refs [12, 23].)

One of the main streamer development problems is explaining the mechanism of the emergence of secondary electron avalanches ahead of the main avalanche. Doing this requires knowing the mechanism of the emergence of secondary electrons. This mechanism is commonly related to either the photoionization of gas, as was initially assumed by the originators of the streamer discharge theory [16, 19, 26], or to electrons that have velocities higher than v and escape from the avalanche head to ionize neutral gas particles [22, 24]. We consider each of these mechanisms in greater detail.

The photons emitted by excited molecules from the avalanches in a gas have a marked effect on the mechanism of gas discharge. The avalanche radiation results in the photoionization of the gas and the photoeffect at the cathode, thereby producing secondary electrons. Direct measurements of the avalanche emission spectra with the aid of a vacuum spectrograph [28] showed that intense lines in oxygen have wavelengths $\lambda = 988$, 880, and 835 Å. Lines with wavelengths below 1000 Å were recorded in nitrogen.

The emission of ionizing radiation is characterized by the following parameters: ω [cm^{-1}], the number of gas-ionizing photons produced by an electron over a path of 1 cm; δ [cm^{-1}], the total number of photons produced by an electron over a path of 1 cm; and ω/α, the number of ionizing photons per electron in the avalanche.

The parameters of ionizing radiation were measured in Refs [20, 21]. For a radiation source, an incomplete discharge in a homogeneous field was used. This permitted tracing the E/p-dependence of different radiation parameters in the gas discharge. In pure oxygen, ω/p was found to increase with E/p, which is attributable to the shortening of the radiation wavelength with increasing E/p.

In air, the ionization potential of oxygen is ~ 3.5 eV lower than that of nitrogen, and therefore the photons emitted by nitrogen ionize oxygen. With increasing E/p, the collisional ionization coefficient α for air increases faster than the ω coefficient, and therefore the magnitude of ω/α decreases with increasing E/p [21].

It follows from Ref. [29] that every avalanche electron in air produces on average 0.4 photons at the pressure $pd = 20-120$ cm Torr ($d = 1$ cm), wavelength $\lambda > 2000$ Å, and $E/p = 50-80$ V cm^{-1} Torr^{-1}. Excited gas molecules emit photons in a time t_{ex} on average. With increasing the gas pressure, the value of t_{ex} shortens owing to excitation-quenching collisions. According to the data in Ref. [30],

$$t_{ex} = t_0 \left[1 + \frac{p}{p_0}\right]^{-1}$$

for nitrogen, where $t_0 = 36 \pm 3$ ns and $p_0 = 60 \pm 6$ Torr.

The authors of Refs [31, 22] pointed to the probable participation of the electrons of the primary electron avalanche in the formation of secondary avalanches. This applied to the electrons in the avalanche head that were forced out by the electrostatic field of electrons. This effect was used to interpret the mechanism of air discharge in ultrastrong electric fields (up to 10^6 V cm^{-1}). In Ref. [32], an attempt was made to construct the streamer theory by invoking the idea of runaway electrons, which were discovered in Ref. [33] earlier. The electrons in the low-temperature weakly ionized plasma of a gas discharge acquire the energy of ordered motion from the electric field and spend it primarily for ionizing and exciting neutral particles. For a high electric field strength – pressure ratio, the energy gained by the electron over a unit path length may exceed the energy imparted in inelastic collisions, and the electron therefore moves to the regime of continuous acceleration.

Reference [32] involved the following qualitative reasoning. Because the electrons in the avalanche head have different energies, including those significantly higher than the average energy ε_{av}, these electrons can escape from the avalanche towards the anode to find themselves in the enhanced-field domain. Part of the electrons that have insufficiently high initial energy slow down in the gas, while higher-energy electrons can gain even higher energy of ordered motion in the enhanced-field domain and travel in the regime of continuous acceleration, even though the field becomes weaker. We return to the issue about the role of runaway electrons in Section 5.2.

4. Temporal characteristics in multielectron initiation

4.1 Breakdown formation time τ and the similarity law

Fletcher [27] has experimentally measured the breakdown formation time τ at atmospheric pressure in air with the use of nanosecond pulses. He showed that the time τ for gaps belonging to the millimeter range in the field $E > 50$ kV cm^{-1} depends only on the value of E and not on the voltage U and the gap length d separately. These data therefore corroborate the validity of the similarity law. The $\tau(E)$ dependence for atmospheric air pressure obtained in Ref. [27] is described by formula (40) with $N_c = 10^8$ (Fig. 6), i.e., as in a conventional streamer discharge in atmospheric air for $d \simeq 1$ cm. It was just what the author of Ref. [27] supposed: that the discharge is initiated by individual electrons and the discharge is a streamer.

The experimental technique used in Ref. [27] was as follows. A voltage pulse with the rise time 0.3 ns was fed via a coaxial line. The cathode and the anode were located at the boundaries of a cut on the inner conductor (Fig. 7a). Figure 7b shows the equivalent circuit of the experimental facility. The discharge formation time τ was measured from the instant the rising pulse voltage reached a value U_a to the instant the voltage across the gap was a few percent lower (Fig. 7c). Consequently, the onset of a decrease in the voltage across the gap and of current growth was taken for the breakdown criterion. The cathode was illuminated with an ultraviolet spark to produce initiating photoelectrons.

We enlarge on several contradictions in Ref. [27], which refute the streamer nature of the discharge under investigation. First, the experiments by the author himself indicate that the discharge is not a streamer [27]. For instance, the distribution $|\ln(n_t/n_0)| = f(t)$ given by the author for $d = 1.55$ mm and $E = 82$ kV cm^{-1} (a double overvoltage)

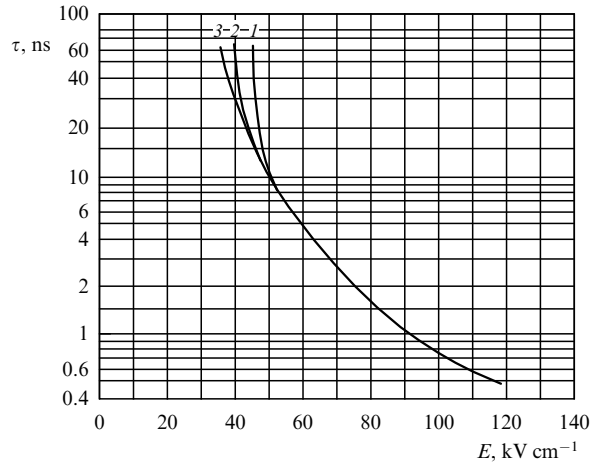

Figure 6. Discharge formation time τ as a function of the field strength E for an atmospheric air discharge; curve *1* was obtained for the pulse amplitude 7.5 kV, curve *2* for 12.7 kV, and curve *3* for 18 kV.

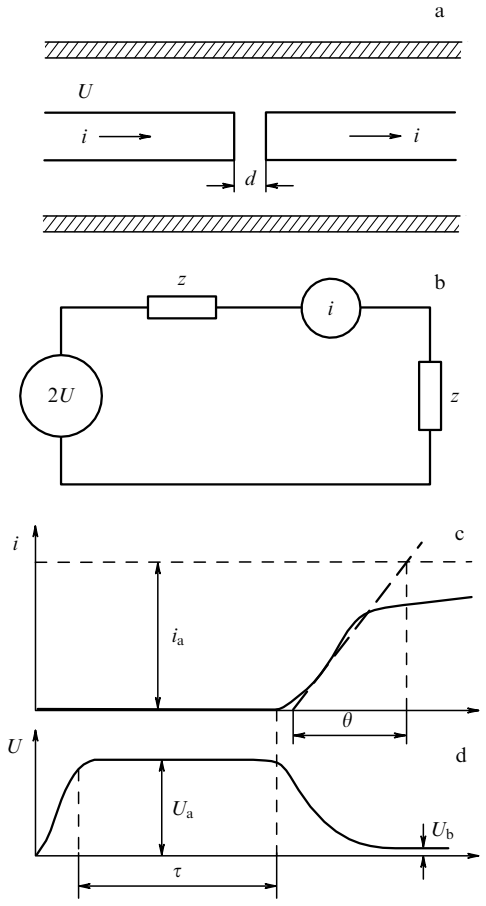

Figure 7. (a) Diagrammatic representation of an experimental facility in which a discharger with a gap d is built into a coaxial line. (b) Equivalent electric circuit of the facility: $2U$ — voltage generator, $i = (Nev)/d \exp(\alpha v t)$ — current generator, z — wave impedance of the coaxial line. (c) Oscillogram of the current discharge. (d) Schematic sketch of the voltage across the gap during the discharge.

shows a wide scatter in the times τ even when more than one electron was certainly at the cathode. This scatter was eliminated when the ultraviolet cathode-illuminating flash was made 60 ns prior to the voltage pulse arrival and produced the current 1.7×10^{-8} A from the cathode, which corresponds to about $N_0 = 10^4$ electrons at the cathode prior to the pulse arrival at the gap. Along with the widening of the scatter with a decrease in the number of electrons at the cathode, the shortest time in the distribution $|\ln(n_t/n_0)| = f(t)$ also changes, which is commonly taken as the discharge formation time τ. The dependence of τ on the number of initial electrons at the cathode was also demonstrated in Refs [31, 34], where the number of electrons N_0 was controlled by varying the time between the ultraviolet spark radiation flash and the arrival of the pulse. The dependence of τ on the number of electrons from the cathode may also be judged by the data in Ref. [35], where the values obtained for τ were approximately two times larger than in Ref. [27], because it may be assumed from the description of the technique in Ref. [35] that the value of N_0 was lower than in Ref. [27].

Second, the formation time τ in Ref. [27] was determined from the oscilloscope traces of the current, whose amplitude was in the range of several hundred amperes. Considering that the onset of current growth in the gap, up to which the time τ was measured, may be fixed for the current through the gap about 1A, the number of electrons in the avalanche for the drift velocity $v \approx 10^7$ cm s^{-1} should amount to $\sim 10^{11}$ and not 10^8, which follows from the streamer theory.

Third, the existence of a one-avalanche streamer discharge is not corroborated by direct observations of the discharge structure with the aid of high-speed photography in the nanosecond range [36, 12]: in this case, the entire gap volume is observed to glow from the instant of voltage application for a time τ and in the stage of fast current buildup, and there is no local radiating object characteristic of a streamer [19]. The fact of the volume glowing is also directly confirmed by gap photographs recorded during the discharge on application of a single nanosecond pulse [12].

To interpret the $\tau(E)$ curve plotted in Fig. 6, Dickey [37] calculated the transient process in the discharge circuit (Fig. 7b) for a single initiating electron under the assumption that the number of electrons in the avalanche may be arbitrarily large. In this case, he obtained the time interval from the onset of voltage application to the onset of current buildup and voltage decrease, which was taken as the time τ in Ref. [27], and this time interval turned out to be longer than that obtained in Ref. [27]. What is most important, he showed that the steepness of the voltage decrease and, accordingly, of the current increase agrees nicely with that measured from the oscilloscope traces in Ref. [27] (Fig. 8).

But this explanation is incorrect because in a space void of charges, the current in the gap must be closed due to the displacement current. In this case, the experimentally observed $\sim 10^2$ A current may be due to either the large capacitance of the gap or the high growth rate of the capacitance in the course of avalanche motion.

The intrinsic gap capacitance is normally of the order of several picofarads, which is insufficient to transmit a current of 10^2 A even for the growth rate 10^{11} A s^{-1}. For the pressure $p = 760$ Torr and $E/p = 150$ V cm^{-1} Torr^{-1}, the quantity $\alpha/p = 1.6$. For the number of electrons in the avalanche to become as high as $\sim 10^{13}$, it should therefore traverse a path $x \approx 0.26$ mm, and therefore this capacitance would remain almost invariable for $d > 3$ mm.

Furthermore, as shown in Section 3.3, for some number N of electrons in an avalanche (for $E/p = 40$ V cm^{-1} Torr^{-1} $N \approx 10^8$), the effect of the space charge field is so strong that

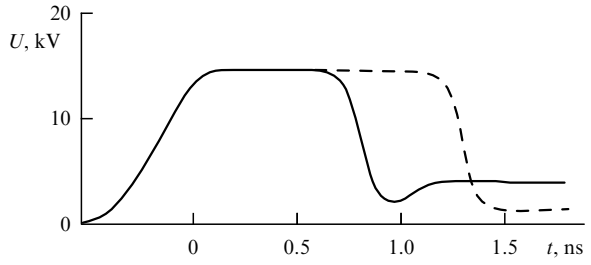

Figure 8. Oscilloscope trace of the voltage across the gap (solid curve) and voltage calculated in the framework of the avalanche electron multiplication model (dashed curve) for $N_0 = 1$. The gap length $d = 1.37$ mm, $E = 104.4$ kV cm^{-1}.

neglecting it leads to even greater errors. Moreover, the avalanche completely ceases developing due to the slowing-down by the space charge [26]. That is why the physical interpretation of the data in Ref. [27] given in Ref. [37] is unconvincing. However, it is amazing that the time dependences of the voltage during the voltage decrease obtained in Ref. [37] are in good agreement with the oscilloscope traces in Refs [27, 31]. The reason why this contradiction occurs is explained in Section 4.3.

Felsenthal and Proud [38] investigated a nanosecond pulsed discharge in different gases using a technique similar to that in Ref. [27]. In this case, the initial number of initiating electrons was also of the order of 10^4. These experiments were carried out under the following conditions: the voltage $E = 4-30$ kV, the gas pressure $p = 1-760$ Torr, the interelectrode gap $d = 0.05-6$ cm, and the discharge formation time $\tau = 0.3-30$ ns. The validity of the similarity law under these conditions was proven for nine gases (Fig. 9).

An explanation why the similarity law applies to the pulsed gas breakdown with multielectron initiation was provided by Mesyats [31] and his collaborators [12, 39]. For a large number N_0 of initial electrons, the current builds up due to the simultaneous development of a large number of electron avalanches. To calculate the dependence of $p\tau$ on E/p, we use the equivalent circuit of the discharge circuit

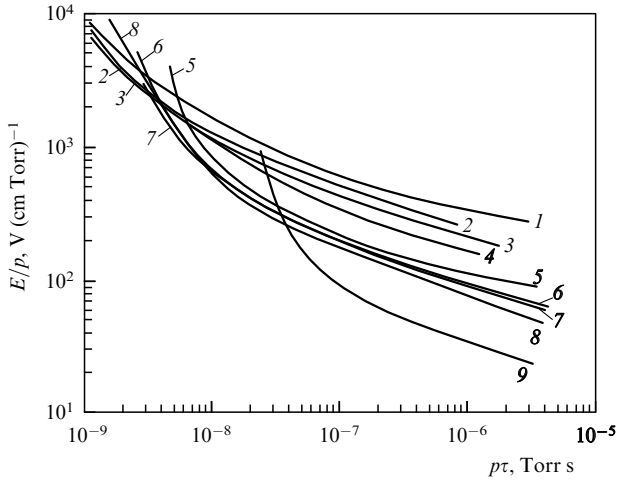

Figure 9. Breakdown formation time as a function of the electric field strength E and pressure p for different gases. *1* — freon-S318; *2* — freon-114; *3* — freon-12; *4* — SF_6; *5* — N_2; *6* — air; *7* — O_2; *8* — Ar; *9* — He.

(Fig. 7b) in the experiments in Refs [27, 38, 39]. The spark gap is replaced with a current generator, which depends on the way of producing the initiating electrons. When these electrons are produced at the cathode and their number is N_0, we have

$$i = \frac{N_0 e v}{d} \exp\left(\int_0^t \alpha v \, \mathrm{d}t\right), \tag{43}$$

where e is the electron charge, d is the gap length, and v the electron drift velocity. When the initiating electrons are produced throughout the cathode and the anode, we have

$$i = n_0 e v S \exp\left(\int_0^t \alpha v \, \mathrm{d}t\right), \tag{44}$$

where S is the surface area of the electrodes and n_0 is the initial electron density between the electrodes. On the other hand, if the gap capacitance is neglected, the current can be determined from the Kirchhoff equation

$$i = \frac{U_a - U}{z} = \frac{d}{z}(E_a - E), \tag{45}$$

where U_a and E_a are the respective amplitudes of the voltage and the field intensity and z is the wave impedance of the coaxial line. Formula (45) takes into consideration that the generator voltage in the equivalent circuit (Fig. 7b) is equal to $2z$ and the total resistance is $2U$. We assume that the pulse has a perfectly rectangular front.

The discharge formation time τ in this case is determined by the time interval between the instant of voltage application and the onset of a decrease in the voltage across the gap and of the buildup of current through the gap. We fix this instant as the moment the current attains a value $i_\tau \ll U_a/z$. From formula (43), we then obtain

$$\tau = \frac{1}{\alpha v} \ln \frac{i_\tau d}{e N_0 v}. \tag{46}$$

If it is assumed that $i_\tau = 1$ A, $d = 1$ cm, $v = 10^7$ cm s^{-1}, and $N_0 = 10^4$, the quantity in the logarithm is $\sim 10^8$, which is equal to the value of N_c obtained in Ref. [27] under the assumption that the streamer discharge mechanism occurs. The quantity appearing in the logarithm in formula (46) has only a weak effect on the time τ, and therefore the similarity law may be considered applicable in the case of multielectron initiation of the pulsed discharge. One more contradiction of Refs [27] and [37] is explained. Because the number of initiating electrons is $N_0 = 10^4$ and it was assumed in Ref. [37] that $N_0 = 1$, this is precisely the circumstance that underlies the difference between the curves in Fig. 8.

However, as is evident from Fig. 6, the $\tau(E)$ dependence in atmospheric air for relatively low fields departs from the similarity law. This is attributable to the fact that the total current of the avalanches that reach the anode is lower than the current i_τ taken to determine the time τ. The condition that determines when such departures are to be expected is written as $d < \tau v$, and hence, in view of formula (46), it follows that

$$d < \frac{1}{\alpha} \ln\left(\frac{i_\tau d}{e N_0 v}\right). \tag{47}$$

For ease of comparing condition (47) with experimental data, we multiply the left- and right-hand sides by E_a. We then obtain

$$U_a < \frac{E_a}{\alpha} \ln\left(\frac{i_\tau d}{eN_0 v}\right). \quad (48)$$

Substituting α given by formula (18) in inequality (48), we obtain the expression for the E/p value below which the similarity law is violated,

$$\frac{E}{p} = B\left[1 + \frac{M}{2U_a} + \left(\frac{M}{U_a} + \frac{M^2}{4U_a^2}\right)^{1/2}\right], \quad (49)$$

where $M = (1/A_0B_0)\ln(i_\tau d/eN_0 v)$. The violation of the $E(t)$ dependences in the experiments in Ref. [27] was observed for $U_a = 12.7$ and 7.5 kV. We substitute these values in formula (49) to obtain the respective electric field strengths 42 and 51 kV cm^{-1}. The respective experimental values of these quantities in [27] are 42 and 50 kV cm^{-1}. This testifies to a satisfactory theoretical explanation of the departure of the $\tau(E)$ dependence from the similarity law. We recall that this occurs in short gaps ($d \sim 1.5-3$ mm).

Therefore, the similarity law for the time τ in multielectron initiation may be considered valid in the 10^{-10}–10^{-7} s range. One more confirmation of this statement is provided by Ref. [40], where the dependence of the time τ on the pressure of argon is investigated for $p = 0.5-600$ Torr. The $\tau(p)$ curve was shown to have a minimum, $\tau_{min} = 250$ ns, for the pressure $p_{min} = 100$ Torr. The existence of such a minimum was earlier indicated in Ref. [41]. We show that the occurrence of this minimum is, according to our theory, in complete agreement with the similarity law. For argon, in a wide range of E/p, we have the dependence [42]

$$\frac{\alpha}{p} = A\exp\left(-\frac{B}{(E/p)^{1/2}}\right), \quad (50)$$

where $A = 33$ (cm Torr)$^{-1}$ and $B = 22.7$ V$^{1/2}$ (cm Torr)$^{-1/2}$. We write the electron drift velocity in the general form

$$v = c\left(\frac{E}{p}\right)^{\varkappa}, \quad (51)$$

where c and $\varkappa$ are parameters that depend on the sort of gas and the E/p value range. Then, substituting formulas (50) and (51) in formula (46) and assuming that the numerator depends only slightly on E/p because it occurs in the logarithm, we find the minimum from the relation $d\tau/dp = 0$. We then obtain the pressure at which the time τ is minimal as

$$p_{min} = \frac{E}{B^2}. \quad (52)$$

It follows from formula (52) that at the minimum point, $(E/p)_{min} = B^2 = 515$ V (cm Torr)$^{-1}$. According to Fig. 9, this value of E/p corresponds in argon to $(p\tau)_{min} = 2\times10^{-8}$ Torr s. The experimental value is $(p\tau)_{min} = 2.5\times10^{-8}$ Torr s. Considering that the pulse in Ref. [40] is not strictly rectangular, the theoretical value of $(p\tau)_{min}$ may be thought of as being in satisfactory agreement with the experimental one. This supports the conclusion that the similarity law for a gas discharge holds for times $\tau \ll 10^{-9}$ s, i.e., for the picosecond range.

4.2 Current buildup and voltage drop time θ

It is easily shown that in the multielectron initiation, the current buildup time and, accordingly, the drop time for the voltage across the gap, which is equal to the former, are determined, like the time τ, by the ionization multiplication of electrons and their drift velocity. Let the gap under investigation be connected in series with a coaxial line (Fig. 7a). This circuit corresponds to the equivalent circuit depicted in Fig. 7b. Then, according to the Kirchhoff law, the relation between the current i and the voltage U is described by Eqn (45). We simultaneously solve Eqns (43) and (45) to obtain [31]

$$\frac{dU}{dt} = -\left(1 - \frac{U}{U_a}\right) U\alpha v. \quad (53)$$

Equation (53) may be written in the framework of the similarity law as

$$\frac{d(E/p)}{d(pt)} = -\left(1 - \frac{E/p}{E_a/p}\right)\frac{E}{p}\,\frac{\alpha}{p}\,v(E/p). \quad (54)$$

Consequently, in the multielectron initiation, the similarity law applies not only to the discharge formation time τ but also to the time during which the drop in voltage across the gap and, accordingly, the buildup of current through the gap occur. It is evident from formula (54) that the field $E(t)$ is independent of the initial number N_0 of initiating electrons. This explains why the calculations performed in Ref. [37] for $N_0 = 1$ yielded the same $U(t)$ decreasing-voltage dependence as for $N_0 = 10^4$ in Ref. [27, 31] (see Fig. 8).

We now estimate the time of the current growth and the voltage drop across the gap. The collisional ionization coefficient α/p is approximated by formula (18) and the electron drift velocity is defined by formula (42) for $\varkappa = 1$ and $c = 3.3\times10^5$ cm^2 Torr V^{-1} s^{-1}; it then follows from Eqns (45) and (53) that

$$\frac{dx}{dT} = (1-x)^2(x-B)\,x, \quad (55)$$

where $x = i/(U_a/z) = 1 - U/U_a = 1 - y$, $B = 1 - 27.5/(E/p)$, $T = t/t_0$, $t_0 = 42p^{-1}(E_a/p)^{-3}$, and $y = U/U_a$. The time dependences of the relative discharge current $x = i/i_a$ for different E/p, which were calculated in our work [31], are plotted in Fig. 10. It follows from these dependences that the curve $x(t)$ initially rises steeply and then its growth is strongly moderated. The fast-to-slow growth transition is attributable to the fact that the voltage drop across the resistance increases with an increase in the current, which results in a lowering of the field strength in the gap and a decrease in the collisional ionization coefficient α and the electron drift velocity v. The last-mentioned circumstance lowers the rate of current growth.

In the steep part of the $x(t)$ curve, the slope $\dot{x} = dx/dt$ is steepest for $x = x_{max}$. The value of x_{max} is determined from the condition $d^2x/dT^2 = 0$:

$$x_{max} = 0.1\left[3(B+1) - \sqrt{9(B+1)^2 - 20B}\right]. \quad (56)$$

By calculating the values of $\dot{x}_{max}(B)$, it is possible to determine the dependence of the time $\theta = i_a(di/dt)^{-1}_{max}$ on E_a/p. The quantity $x_{max}(B)$ and the corresponding dependence of the derivative $\dot{x}_{max} = (dx/d\tau)_{max}$ on B are plotted in

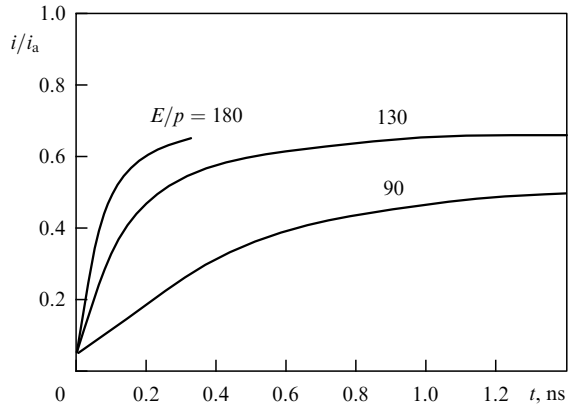

Figure 10. Time dependences of the current in atmospheric air for different E/p values calculated in the framework of multiavalanche electron multiplication.

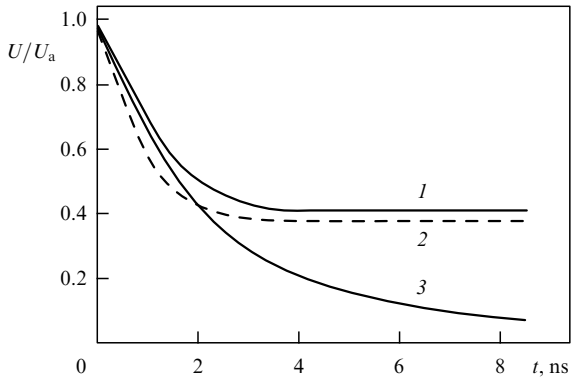

Figure 12. Experimental (*1*) and calculated (*2*) oscilloscope traces of decreasing voltage in the multielectron initiation of nitrogen breakdown ($p = 760$ Torr, $d = 0.44$ cm, $E = 68.5$ kV cm^{-1}) and experimental oscilloscope trace of the voltage decrease in the one-electron initiation (*3*).

Fig. 11. Using the curve $\dot{x}_{max}(B)$, it is possible to find the dependence of $\theta = i_a(di/dt)^{-1}_{max}$ on E_a/p. It is easy to demonstrate that the similarity law holds for the conventional time θ of voltage drop and the increase in the current (see Fig. 7c)

$$p\theta = \frac{0.024}{(E_a/p)^3 (dx/dT)_{max}}, \tag{57}$$

because $\dot{x}_{max} = (dx/dT)_{max} = f(E_a/p)$. The measured values of θ for three gap lengths $d = 1, 2$, and 4 mm for multielectron and one-electron initiation fit well into this curve [31].

In the one-electron discharge initiation, there are also two parts in the curve of voltage decrease: a fast and a slow decrease. Figure 12 shows the experimental dependences $U/U_a\,(t)$ for the multielectron and one-electron initiation, as well as the theoretical curve. It is pertinent to note that by determining the time θ, we have characterized only the initial, steep portion of the voltage decrease curve. But a second portion also exists with a relatively slow voltage decrease, which is recorded in the oscilloscope trace as a 'footstep.' This permits naming it the residual voltage or the operating voltage, U_b, of a volume discharge. This footstep occurs because as the current increases, the average field E in the gap decreases and, accordingly, the values of α and v decrease, resulting in a strong moderation of the decrease in the voltage across the gap. We assume that

$$\frac{dU_b}{dt} \ll \left(\frac{dU}{dt}\right)_{max}$$

and that the voltage U_b is attained when $dU/d(pt) = h_0$, where h_0 is some quantity that is small in comparison with the maximum steepness. As is easy to show, with the electron velocity $v = c(E/p)$, it follows from Eqn (53) that

$$h_0 = \frac{U_b^2}{pd}\left(1 - \frac{U_b}{U_a}\right) f\left(\frac{U_b}{pd}\right). \tag{58}$$

As is evident from formula (58), the discharge operating voltage is independent of the wave impedance z of the generator. With this definition of the operating voltage U_b, the similarity law $U_b = \varphi(pd)$ is upheld according to formula (58). For $U_a \gg U_b$, the dependence of U_b on U_a is weak, i.e., U_b remains practically the same for different initial voltages. Figure 11 gives the experimental and theoretical dependences of $y = U_b/U_a$ on E_a/p for atmospheric air for the steepness dU/dt five time smaller than the maximum steepness. This discharge stage is commonly used for pumping gas lasers and in plasmotrons.

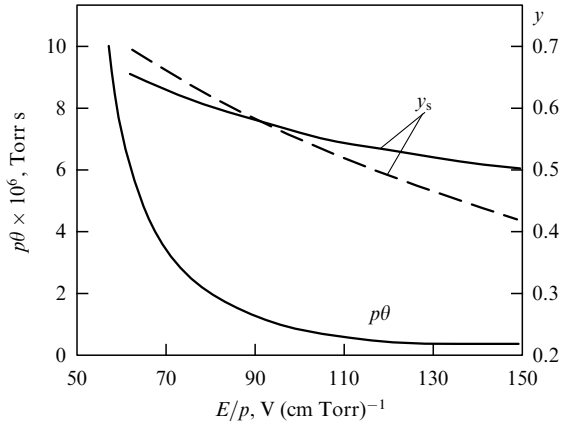

Figure 11. $p\theta$ for multielectron and one-electron initiation and the relative voltage y_s for which the steepness of voltage decrease is one fifth the maximum steepness, as functions of E/p for different air gaps of lengths 1, 2, and 4 mm. Solid curves show the theoretical data and the dashed curve corresponds to the experimental data obtained for air at $p = 760$ Torr.

5. One-electron initiation

5.1 Breakdown formation time τ and the current-buildup and voltage-drop time θ in the one-electron initiation

In air gaps of length $d \leqslant 1$ mm, in the initiation of discharge by single electrons (one-electron initiation), the similarity law is violated and the time τ becomes one or two orders of magnitude longer than expected from the data for discharges with the multielectron initiation.

It was proven in Ref. [39] that the time τ depends on the number N_0 of initial electrons. Voltage pulses up to 30 kV in height with the rise time 0.3 ns were used. The discharge chamber was filled with air at atmospheric pressure. There was an opening in the anode, which was covered with a copper

mesh. The gap length $d = 2$ mm remained invariable. The ultraviolet cathode was illuminated with a miniature spark source; its radiation was incident on the cathode at 90° via a quartz lens, an aperture stop, and the anode mesh. The aperture stop enabled changing the irradiation area by a factor of 10^3, the lens transmitted radiation with wavelengths no shorter than 2000 Å to the cathode, which ruled out the photoionization of gas. The facility enabled realizing both one-electron and multielectron initiation. The multielectron initiation was realized when the ultraviolet radiation arrived significantly earlier than the main voltage pulse. The one-electron initiation was effected when the radiation arrived 10 ns after the arrival of the main pulse at the gap. The possibility that an initiating electron emerged during this period was excluded because the delay time for a discharge without illumination was always longer than 100 ns.

For each pulse amplitude, 100 oscilloscope traces were recorded to plot the dependences $|\ln(n_t/n_0)| = f(t)$, where n_t is the number of breakdowns with the time delay t or longer and n_0 is the total number of breakdowns. For example, Fig. 13 shows two of these distributions for $E = 100$ kV cm^{-1} and $E = 90$ kV cm^{-1}. The shortest time in this distribution was taken as the time τ. The cathode irradiation intensity was chosen such that the time σ was comparable to τ. This practically excluded the simultaneous emergence of two electrons whose avalanches might interfere with each other.

The dependence of the time τ on the field E_0 obtained for one-electron initiation is shown in Fig. 14 (curve *3*). Also given in Fig. 14 are curve *1* obtained in Ref. [27] and the results in Ref. [39] for multielectron initiation (the data points in curve *1*). In the latter case, the illumination commenced 100 ns earlier than the pulse and the intensity of ultraviolet cathode irradiation was approximately 100 times higher than the intensity when recording the curves given in Fig. 13. The number of electrons accumulated at the cathode was therefore $\sim 10^4$, as in Ref. [27]. The values of the time τ measured in this case coincide with the data in Ref. [27]. Curve *2* was obtained in Ref. [35] under conditions close to one-electron initiation.

It can be seen from Fig. 14 that the discharge formation time substantially depends on the number of breakdown-

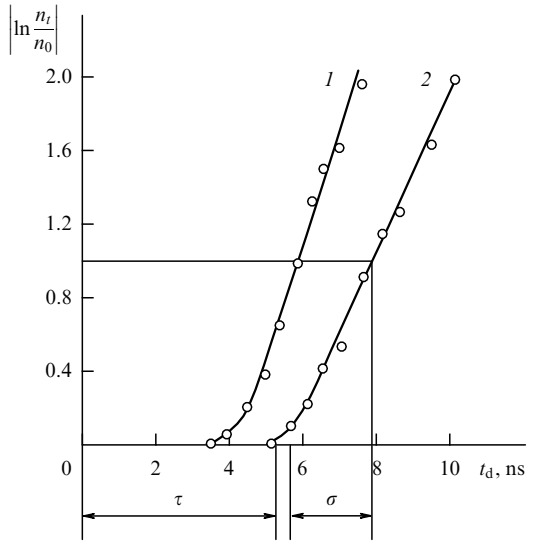

Figure 13. The distribution $|\ln(n_t/n_0)| = f(t)$. Curve *1* — $E = 100$ kV cm^{-1}, $d = 2$ mm, curve *2* — $E = 90$ kV cm^{-1}, $d = 2$ mm.

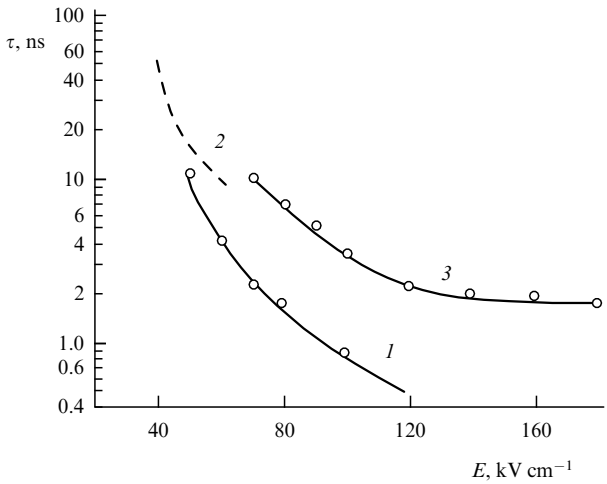

Figure 14. The formation time τ versus the field E. Curve *1* was plotted using the data in Ref. [27]: the points were obtained for the multielectron breakdown initiation [31]; curve *2* corresponds to the data in Ref. [35] for the one-electron initiation; curve *3* is the dependence obtained for the one-electron initiation [31].

initiating electrons. All known experimental facts can be explained by assuming that the onset of the fast current growth and the decrease in the voltage across the gap, which is commonly recorded as the instant of breakdown, are due to the development of electron avalanches initiated by free electrons in the gap. For a large number N_0 of initiating electrons during the time τ that is commonly taken as the discharge formation time, the current of these avalanches builds up to some value i_τ that can be recorded with an oscilloscope. When the number N_0 of electrons is small, e.g., $N_0 \approx 1$, free electrons are accumulated in the gap during the discharge formation stage due to secondary processes.

An investigation of a nanosecond pulsed atmospheric air breakdown for the one-electron initiation in gaps of length $d < 1$ mm was carried out in Ref. [34]. The electric field in the breakdown amounted to 10^6 V cm^{-1}. No ultraviolet cathode illumination was effected, and the initiating electrons were produced due to the field emission current. As shown in Ref. [34], in the case of a careful cleaning and polishing of the electrodes, for the gap length $d = 0.1$ mm and the electric field $E = 1.4 \times 10^6$ V cm^{-1}, the time $\tau \approx 1$ ns. Scratching the cathode surface had the effect that the time τ shortened to values $\tau < 10^{-10}$ s. This is attributable to the fact that the discharge went over into the multielectron initiation mode initially due to the field emission current and subsequently due to explosive electron emission from the micropoints on the cathode surface, which emerged at the edges of the scratch.

The relatively long τ in the discharge initiation by a small number of electrons may have several possible causes, all due to the deficiency of the number of electrons in the gap, which prevents the discharge current from rapidly attaining a value perceived as a discharge. First, because of the good cathode processing, the number of initiating electrons is small: on the cathode, there are few micropoints at which the electric field is enhanced to increase the field emission current. Second, for fields $E > 10^5$ V cm^{-1}, the effect of electron avalanche self-braking becomes much stronger. That is, the growth rate of the number of electrons in the avalanche decreases sharply for the number of electrons $N \approx 10^6$ in the path $x_c \ll d$. Naturally, few excited neutral particles are produced in such

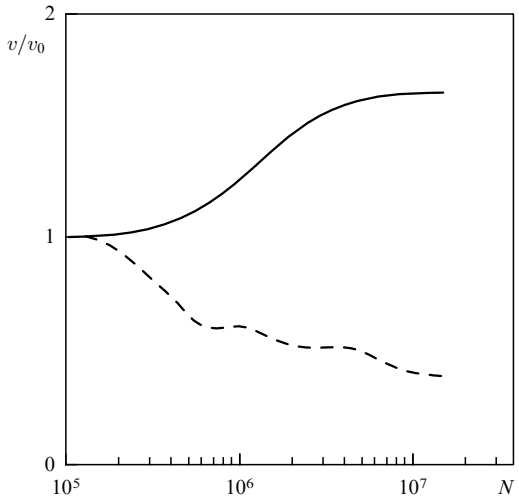

Figure 15. Electron velocities at the front (solid curve) and at the tail (dashed) of an avalanche as functions of the number of charges in the avalanche; v — the current electron drift velocity, v_0 — the initial electron velocity.

an avalanche, and it emits few photons or runaway electrons (REs). That is why a streamer cannot arise in the gap. Third, owing to the small number of photons emitted by the avalanche, few photoelectrons are produced at the cathode. All this is responsible for a sharp decrease in the growth rate for the number of free electrons in the discharge gap.

For fields $E > 10^5$ V cm^{-1}, the avalanche itself exhibits significant distinctive features: it experiences strong distortion. The velocity of electron motion at the avalanche front is substantially higher than at its tail [23] (Fig. 15), i.e., the electrons are ejected from the avalanche front. Together with REs, these electrons produce a new avalanche ahead of the front of the primary avalanche. A plasma object termed the avalanche chain thus emerges [22]. On bridging the gap, the avalanche chain does not give rise to a sharp increase in the current owing to its very low conductivity. But it emits photons, which produce new electrons at the cathode and in the gas due to photoemission from the cathode and thereby produce new avalanche chains. This mechanism resembles the Townsend mechanism, with the difference that the role of a separate avalanche is played by an avalanche chain. In this situation, the time τ depends on the de-excitation time of excited atoms and molecules. In particular, for nitrogen at $p = 760$ Torr, as shown in Section 3.3, this time is equal to 2.5 ns. Naturally, the similarity law for the time τ does not hold for the one-electron initiation under these conditions.

The field emission, the avalanche chain development, the emergence of REs, and the production of photoelectrons are responsible for the accumulation of the number of electrons in the gap such that the increase in the discharge plasma conductivity and the decrease in voltage across the gap occur during one avalanche generation time. Interestingly, the initial stage of this decrease is the same as in the multielectron initiation. This is attested by curve *3* plotted in Fig. 12, which shows the decrease in the voltage across the gap in the one-electron initiation. It can be seen from Fig. 12 that the time θ is independent of the number of initiating electrons.

The structures of plasma glow in the gap in multi- and one-electron initiation are substantially different. While the entire gap glows in the former case, numerous diffuse channels linked to different points on the cathode are observed against the weak volume glow in the latter case. This structure of atmospheric air discharge was first discovered by the authors of Refs [31, 43] and more recently by other authors [24, 44]. These points on the cathode are the sites of field emission enhancement.

The volume glow is due to the photoemission from the cathode and the photoionization of gas by the photons emanating from diffuse channels. The diffuse channels are produced due to the field emission (FE) current from the micropoints on the cathode, at which the electric field may be enhanced by factors of several dozen or even several hundreds [3]. This enhancement becomes even stronger due to the space charge of positive ions. When the electron current density attains a high value, explosive electron emission (EEE) from these micropoints occurs [31, 46], which gives rise to cathode spots and subsequently to brightly glowing discharge channels. The explosive processes at the cathode in a gas discharge were predicted in Ref. [23] and first discovered and investigated in Refs [3, 41, 46, 47]. Their occurrence is directly confirmed by microcraters on the cathode. These are similar to the microcraters that emerge in a vacuum discharge, for which the fundamental role of EEE has been unambiguously proven [48]. There is no question that precisely FE or EEE is responsible for the emergence of REs in a gas discharge gap.

It is interesting to note the effect of channels and bulk plasma in the gap on the discharge. The main current after the onset of the voltage decrease is due to diffuse glow because the initial voltage decrease and current growth time are the same in the cases of multi- and one-electron initiation (see Fig. 12). The subsequent voltage decrease and current growth are governed by processes in the channels. That is why the current increases much faster in the multielectron initiation. This is related to the nonuniformity of electron emission from the cathode surface arising from the large number of micropoints on it. It is the enhanced FE current from the micropoints that leads to the production of diffuse channels. Subsequently, these micropoints explode under the action of the EEE current and discharge channels arise.

5.2 Runaway electrons

In Section 5.1, we investigated the dynamics of air discharge without external preionization sources under electric fields $E \gg 10^5$ V cm^{-1}. Normally observed under these conditions are runaway electrons, as mentioned in Section 5.1. We have already discussed the possible role of REs in the avalanche-to-streamer transition (see Section 3.3) and the production of diffuse channels (see Section 4.2). We now enlarge on the nature of REs and their possible role in the discharges under consideration [3].

Electrons in the low-temperature weakly ionized plasma of a gas discharge acquire the energy of ordered motion from the electric field and spend it primarily to ionize and excite neutral particles. For a large ratio E/p of the electric field strength to pressure, the energy gained by an electron over a unit path length may exceed the energy it loses in inelastic collisions, and the electron can then transit to the continuous acceleration regime.

For a nonrelativistic electron, inelastic energy losses are determined by the well-known formula [49]

$$F(\varepsilon) = \frac{2\pi e^4 n_0 z}{\varepsilon} \ln\frac{2\varepsilon}{I}, \qquad (59)$$

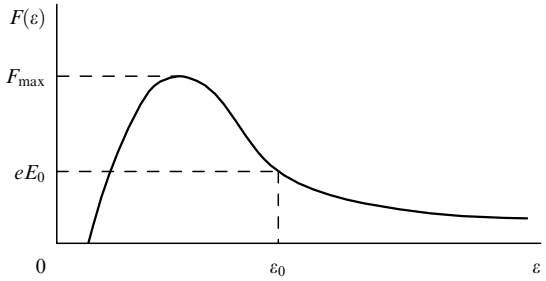

Figure 16. Qualitative form of the energy dependence of the fast-electron braking force in a gas.

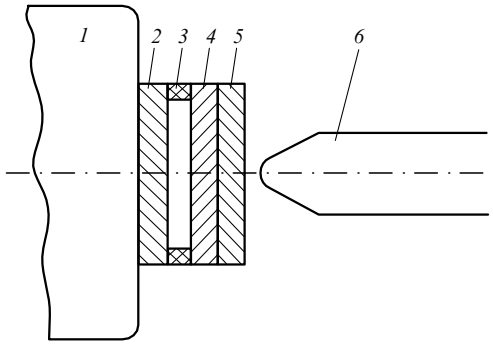

Figure 17. Schematic of the experiment to identify runaway electrons: *1* — photomultiplier; *2* — scintillator; *3* — damper; *4* — absorber; *5* — anode; *6* — cathode.

where n_0 is the density of gas molecules, z is the number of electrons in the molecule, $\varepsilon = mv^2/2$, I is the so-called average energy of inelastic losses, and ε is the thermal electron energy. The value of I is known from experiments. For nitrogen and air, $I = 75-80$ eV, and $I = 44$ eV for helium.

If elastic scattering is disregarded, the electron energy balance for $\varepsilon > I/2$ is written as

$$\frac{\mathrm{d}\varepsilon}{\mathrm{d}x} = eE - \frac{2\pi e^4 n_0 z}{\varepsilon} \ln\frac{2\varepsilon}{I} . \tag{60}$$

The loss function $F(\varepsilon)$ has a peak $F_{\max}$ at the energy $\varepsilon \approx 2.72\, I/2$ (Fig. 16). Hence, it follows that there exists some critical field $E_c = F_{\max}/e$: when the field is above this critical field, electrons with energies $\varepsilon \geqslant I/2$ travel in the regime of continuous acceleration rather than the drift regime. The critical field is given by

$$E_c = \frac{4\pi e^3 n_0 z}{2.72\, I} . \tag{61}$$

Substitution of the corresponding numerical constants in expression (61) gives the condition whereby the electrons in a gas discharge participate in accelerated motion:

$$\frac{E_c}{p} = 3.38 \times 10^3 \, \frac{z}{I} . \tag{62}$$

For instance, $z = 14$, $I = 80$ eV, $E_c/p \approx 590$ V cm^{-1} Torr^{-1} for nitrogen and $z = 2$, $I = 44$ eV, $E_c/p = 154$ V cm^{-1} Torr^{-1} for helium. Similar E/p values are achieved with relative ease at the delay stage of nanosecond pulsed discharges, and continuous electron acceleration should therefore occur in the plasma column of such discharges.

For an electron to move with acceleration in a field E_0, the condition $E_0 \geqslant E_c$ need not be satisfied. Referring to Fig. 16, when an electron has an ordered-motion energy $\varepsilon \geqslant \varepsilon_0$ for a field E_0, $\mathrm{d}\varepsilon/\mathrm{d}x < 0$ and the condition for continuous acceleration is also satisfied.

Runaway electrons in atmospheric air discharges were first observed by Stankevich and Kalinin [33], who carried out several experiments to prove the existence of fast electrons in the initial stage of a pulsed discharge in air at atmospheric pressure. The experiments are schematized in Fig. 17. A voltage pulse 23 ns long with the rise time about 2 ns was imposed across the discharge gap between electrodes *5* and *6*. The bremsstrahlung was incident on organic scintillator *2* via electrode *5* and absorber *4*. The light flash of the scintillator was recorded by a photomultiplier. The photomultiplier together with its power source was enclosed in a metal casing, which shielded the circuit from electromagnetic interference. Test experiments were conducted to confirm that external fields, illumination, and the shock wave had no effect on the circuit.

For the pulse amplitude 46 kV and the positive polarity of electrode *5*, the hardness and intensity of the bremsstrahlung were sufficient to pass through the 2 mm thick aluminum layer (with a 1 mm thick aluminum anode) with a several-fold attenuation; for the amplitude 58 kV, the bremsstrahlung was able to pass through a 0.3 mm thick nickel layer (with a nickel anode). It was not possible to measure the duration of the radiation pulse because it was shorter than the temporal resolution of the setup, equal to approximately 5 ns.

Estimating the radiation intensity showed that the radiation energy about 4×10^{-4} roentgen is liberated per pulse, which corresponds to approximately 6×10^4 photons (for the average photon energy 6 keV). In the view of the authors of Ref. [33], the experiments conducted suggest that electrons in the initial stage of a spark discharge can gain energies comparable to the applied voltage by an order of magnitude.

Noggle et al. [50] observed X-ray radiation in a helium discharge. In these experiments, a Marx generator with the voltage 240 kV and the voltage rise time 10 ns was used. The gap measured 2–10 cm in length, and $E/p = 35-140$ V cm^{-1} Torr^{-1}. The average X-ray photon energy was equal to 10–13 keV. In a series of experiments reviewed in Refs [24, 44, 51], it was possible to directly observe the electrons that emerged through a thin metal foil at the anode.

The experimental conditions in which X-rays were observed were distinguished not only by a high field strength – pressure ratio but also by a high field strength at the cathode. In all old and recent experiments, advantage was taken of a single-pointed cathode or a cylindrical cathode with sharp edges, which in some cases was the end of a helically rolled metal foil [44]. The electric field at the cathode, enhanced due to its sharpness, is said to be the macrofield. However, there are micropoints on the cathode surface that additionally enhance this macrofield by factors of several dozen or even hundred [3]. The electric field at the micropoints is said to be the microfield. The high fields at the cathode surface suffice to give rise to field emission and subsequently explosive electron emission [3]. The existence of this high macrofield is required to satisfy criterion (62), whereby REs emerge. Visual integral photographs show the explosive plasma at the cathode surface. It is therefore invalid to say that we are dealing with REs from discharge streamers

whenever REs are observed. The number of REs in the presence of FE and EEE is always much larger than in the case of a pure gas-discharge effect. The occurrence of explosive processes at the cathode is also attested by spectroscopic investigations of the near-cathode plasma. Observed in air discharges [3, 50] are, as a rule, the spectral lines of nitrogen and of the cathode metal, the latter appearing $\sim 10^{-9}$ s later than the former.

Important information on the nature of REs was gained in the investigation of the beam structure of REs at the anode. The number of diffuse channels [31, 43], as discussed in Section 5.1, was always equal to the number of RE beams [24] recorded at the anode. The investigations revealed that the RE source was either the cathode or the plasma of the cathode flame resulting from EEE. This is evidenced by the following experiment with helium at the pressure 22 Torr [51]. Notches were made on a planar cathode, and the imprints on the anode produced by RE beams corresponded to the notch pattern on the working surface of the cathode. Hence, the REs are caused by the emission due to the existence of micropoints on the notch edges. The spatial distribution of REs in atmospheric air is strongly affected by their scattering by molecules. But experiments with a sharp conic cathode reveal a clear-cut relation between the cathode–anode distance d and the RE beam diameter. For instance, the beam diameter is equal to ~ 6 mm for $d = 5$ mm and to 30 mm for $= 15$ mm. It is pertinent to note that the appearance of the image of structural cathode irregularities on the anode is physically similar to the field emission Müller projector. The flux structure corresponded to the emitting center distribution on the cathode, which is an indication that FE is the decisive factor in the emergence of REs in atmospheric air.

The number of REs varied in the range $N_{re} = 10^8 - 10^{12}$ per pulse, depending on the sort of gas, its pressure p, the overvoltage δ, the cathode geometry, the steepness of the pulse front, and the gap length d. For the pressure $p = 760$ Torr, the gases under investigation can be listed in the order of decreasing N_y: He, Ne, H_2, air, Ar, Xe, and SF_6 [24]. The runaway electrons are emitted in the form of short pulses, which are much shorter than the voltage pulse. According to new, more reliable data, the duration of RE current pulses in atmospheric air is equal to 0.1–0.5 ns [52]. However, these durations are at the resolution limit of oscilloscopes. Conceivably, this quantity might therefore be shorter than 10^{-10} s. For the above number of REs, the 1–100 A amplitudes of current pulses measured in Refs [44, 52] appear to be realistic. This current depends only on the number of emitting centers on the cathode, all other factors being the same. It is therefore unreasonable to compare the RE current for cathodes made in the form of a single point, a metal blade, or a rolled foil.

The most probable source of REs is the FE from the micropoints on the cathode due to the microfield, which lasts from the instant of voltage application to the instant of their explosion. This time is determined by the formula $j^2 t_i = \bar{h}$, where t_i is the duration of the electron current pulse and $\bar{h}$ is the action integral, whose value is equal to $\sim 10^9$ A^2 s cm^{-2} for many metals [48]. For $t_i = 10^{-10}$ s, the electron current density must therefore be equal to $\sim 10^9$ A cm^{-2}. This is achieved for electric field strengths $\sim 10^8$ V cm^{-1} at the micropoints, which is quite realistic [3]. Hence, the duration of RE current pulses is equal to the time delay of micropoint explosions by the FE current.

REs have a rather broad energy spectrum, sometimes having an energy $\varepsilon > eU_a$, where U_a is the pulse amplitude. These electrons were termed anomalous-energy REs. For the air pressure $p = 70$ Torr, $\varepsilon_{max} \approx 200$ keV; for $p = 760$ Torr, $\varepsilon_{max} \approx 300$ keV. With increasing the pressure, the energy spectrum maximum shifts towards higher energies [24].

Therefore, the occurrence of REs in gas discharges has been amply corroborated. We now have to see how they affect the main gas discharge characteristics, which were discussed in Section 4. We first note that all τ values given in Section 4 were measured for a uniform electric field, while all RE measurements were carried out for a strongly nonuniform electric field occurring due to the use of pointed cathodes. Nevertheless, even though the REs may emerge under a uniform electric field, they have no effect of any significance on the value of τ for a multielectron discharge initiation, because the number N_0 of initiating electrons in formula (46) is in the logarithm. As for the magnitude of θ, which determines the decrease time for the voltage across the gap, the number of discharge-initiating electrons does enter Eqn (54) whatsoever. That is why the REs should have little or no effect on the dependences of $p\tau$ and $p\theta$ on E/p.

In the case of one-electron initiation, REs undoubtedly participate in the accumulation of free electrons for a time τ. They are responsible for the emergence of diffuse, weakly conducting channels between the cathode and the anode, part of which transform into high-conductivity channels. These channels determine the eventual spark-to-arc transformation if the voltage is applied for a long time, which underlies the faster decrease in the voltage across the gap in the case of one-electron initiation (see Fig. 12).

6. Pulsed microwave breakdown

In Section 2.3, we discussed a microwave breakdown under continuous voltage application, assuming that the gas being ionized is in a stationary state and that during measurements, the ionization rate follows the electric amplitude, which gradually increases in a quasistationary manner until the production of new electrons slightly exceeds their loss. Then there occur a rapid increase in the electron density and the onset of a breakdown. For a pulsed microwave electric field, no breakdown occurs if the electron density does not reach the critical value prior to pulse cessation. For a pulse generator operation, the breakdown microwave fields would therefore be expected to be higher than for continuous operation, and the breakdown field should depend on the pulse duration and the pulse repetition rate.

It is also evident that a complete analysis of breakdown in the pulsed regime is more complicated than in the continuous regime because the ionization growth rate should be taken into account. However, even without the complete analysis, it is clear that the breakdown fields should be extremely high for very short pulses and that the breakdown field should approach its value in the continuous mode of microwave generators as the pulse duration is increased.

When the microwave generator operates in a pulsed mode, it is more difficult to find a stringent criterion for determining the instant of the onset of a breakdown. In the majority of cases, it is assumed that the breakdown occurs when the electron density in the resonator reaches a value such that an opaque plasma is produced in a time of the order of 5% of the pulse duration [14]. This is attested by a sharp decrease in the energy transmitted through the resonator.

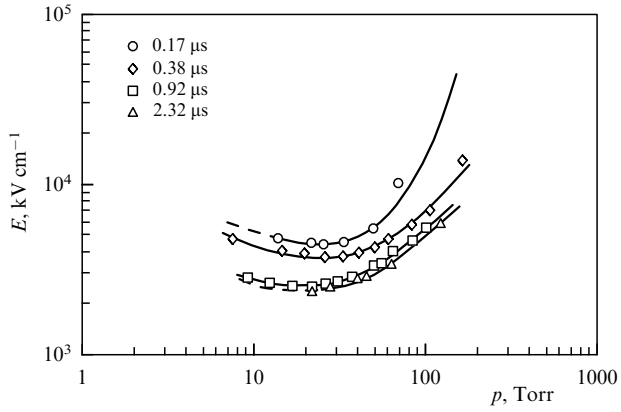

Figure 18. Pulsed air discharge at the frequency 24.1 GHz for $\Lambda = 0.09$ cm, pulse durations from 0.17 to 2.35 μs, and the pulse repetition rate 200 Hz.

A pulsed microwave discharge can be of two types: a single-pulse regime and a periodic-pulse regime. They are distinct only when there are no residual effects (produced by previous pulses) in the plasma or on the chamber walls during the interpulse interval. Figure 18 shows the pressure dependence of the breakdown field strength for atmospheric air at the frequency 24.1 GHz for $\Lambda = 0.09$ cm and the repetition rate 200 Hz for pulses of different lengths [14]. It follows from Fig. 18 that the shorter the pulse, the higher the breakdown electric field strength. With an increase in the pulse repetition rate and pulse duration, the breakdown field strength approaches its values for the continuous regime [14].

We thus see that the similarity law is obeyed in the periodic-pulse regime of the microwave breakdown and the pressure dependence of the breakdown electric intensity has a minimum, as in the stationary regime (see Section 2.3). These dependences are theoretically interpreted in Ref. [53]. But our main concern is whether the similarity law applies to the formation time τ in a single-pulse microwave breakdown. Figure 19 shows the dependence of E/p on $p\tau$ for a microwave breakdown in atmospheric air for different pulse durations. It can be seen that the relation between τ, E, and p for single pulses obeys the similarity law, i.e., E/p is a function of $p\tau$. This fact is explicable on the basis of the simplest theory of microwave breakdown, which assumes that the electron plasma density is determined, on the one hand, by the increase in the number of electrons due to the collisional ionization of neutral particles and, on the other, by the electron loss due to electron attachment and diffusion. When an air breakdown is under discussion, an effective quantity α is commonly used that takes both ionization and attachment into account. In this case, it follows from formula (20) that

$$\ln\frac{n}{n_0} = t\left(v - \frac{D}{\Lambda^2}\right). \tag{63}$$

If it is assumed that the ionization frequency $\nu = \alpha v$ and the breakdown sets in at $t = \tau$, when the plasma density reaches some critical value n_c that characterizes the breakdown, it follows formula (63) that

$$\tau = \frac{\ln(n_c/n_0)}{\alpha v - (D/\Lambda^2)}, \tag{64}$$

where v is the electron drift velocity, D is the diffusion coefficient, and n_0 the initial electron density. According to the electron diffusion theory based on the Maxwellian electron distribution, $Dp = M\varepsilon$, where ε is the thermal electron velocity and M is a constant factor. According to various approximate calculations, this factor is equal to $(3-5) \times 10^5$ for air [14]. The electron energy ε is here taken in Volts, [Torr] is the unit of measurement of pressure, and [$\mathrm{cm^{-1}\ s^{-1}}$] is the unit of measurement of the diffusion coefficient D. It should be borne in mind that $\varepsilon = f(E/p)$.

It follows from formula (64) that

$$p\tau = \frac{\ln(n_c/n_0)}{(\alpha/p)\, v - (Dp/p^2\Lambda^2)}. \tag{65}$$

In view of the aforesaid, formula (65) implies that there is a one-to-one relation between $p\tau$ and E/p for a fixed value of $p\Lambda$, which is confirmed by an experimental curve (see Fig. 19) [53]. We note that in the comparison of theory and experiment, it is commonly assumed that $n_c/n_0 = 10^8$ [38]. This assumption is not substantiated theoretically in any way. The simple fact is that the theoretical results are best fitted to the experimental data for precisely this value.

Interestingly, if the electron diffusion is neglected, formula (65) for $n_c/n_0 = 10^8$ transforms into formula (46). This

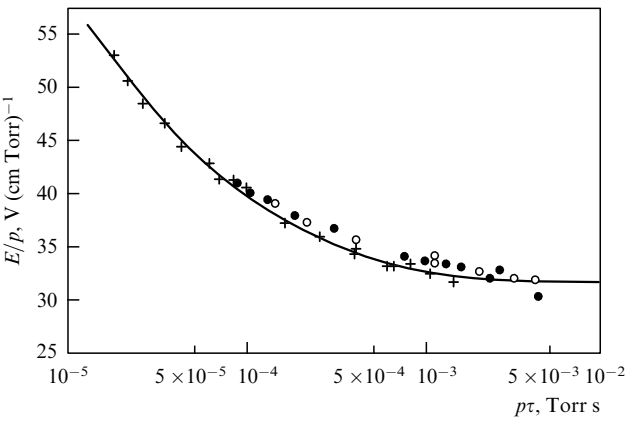

Figure 19. Dependence of the ratio E/p on $p\tau$ for a pulsed microwave air discharge for pulse lengths 0.8 μs (+), 2 μs (•), and 4 μs (○).

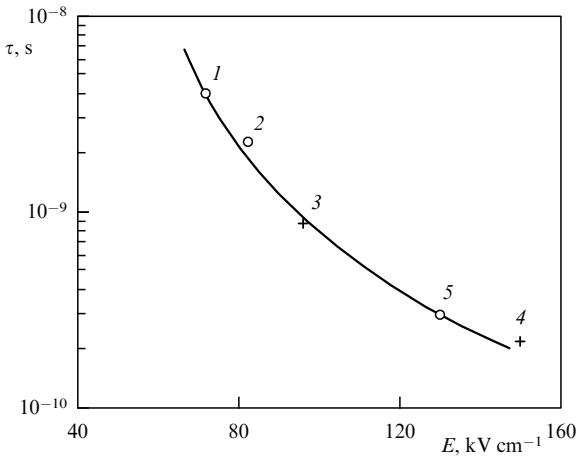

Figure 20. Duration of the voltage pulse versus the breakdown electric field strength: *1*, *2*, *5* — microwave pulses of the 38 GHz frequency range; *3*, *4* — unipolar voltage pulses without microwave filling.

caused the authors of Ref. [38] to come up with the diffusion theory of pulsed gas breakdown under the action of videopulses, although diffusion plays no significant part in such a discharge.

The breakdown field strength for atmospheric air as a function of the pulse length is shown in Fig. 20 for pulse lengths down to 200 ps [54]. Experimental points are given both for videopulses and for radio pulses with the frequency 37 GHz. Also shown is the $E(\tau)$ curve for air at $p = 760$ Torr borrowed from Ref. [27], which confirmed the validity of the similarity law for air in the nanosecond range. It can be seen that the breakdown times for video and radio pulses coincide. This is because only several periods of the microwave oscillations fall within the pulse length, its period being 28 ps. In this case, the electron diffusion is insignificant.

7. Conclusion

Similarity laws play an important role in the physics of electric gas discharges. These laws for breakdown at constant voltage were already established by Paschen and theoretically substantiated in the classical Townsend theory. Similarly, based on the same principles, the similarity law was obtained for a stationary microwave breakdown. The main distinction between these breakdowns is that charged particles (electrons and ions) are eliminated from the gap due to their arrival at the electrodes in the former case and due to diffusion in the latter. The main process is collisional electron ionization of atoms and molecules for both discharges.

The similarity laws are also obeyed for pulsed gas discharges, for both Townsend and streamer discharges. The former occurs for overvoltages not exceeding 10%, the latter for higher overvoltages. For the streamer mechanism, the discharge formation time τ obeys the similarity law of the form $p\tau = f(E/p)$, but for the Townsend mechanism the product $p\tau$ is a function not only of E/p but also of pd. In this case, it is well to bear in mind that the nature of the discharge depends on the gap length and the number of initiating electrons. For air at atmospheric pressure, for instance, the discharge through centimeter-long gaps is of the streamer type for single initiating electrons. In this case, the time τ is determined by the time taken by an avalanche to reach the critical size, when the space charge field becomes comparable to the external field. The avalanche then transforms into a streamer whose velocity exceeds the avalanche electron drift velocity by 1 – 2 orders of magnitude.

For the similarity law to be obeyed in millimeter-long gaps, a large number N_0 of initiating electrons are required, because an avalanche does not reach the critical size over the length d. The number N_0 of initiating electrons should be such that during the electron drift through a gap of length d, the current increases to the extent that a decrease in the voltage across the cathode and the anode sets in. This discharge is termed the discharge with multielectron initiation. Naturally, this discharge may be realized for centimeter-long gaps as well. An important feature of a discharge with multielectron initiation is its volume character, unlike a streamer discharge. The discharge plasma column normally rests upon an area on the cathode where the initiating electrons are located. This is widely used in the pumping of high-power gas lasers. For a streamer discharge, when the streamer bridges the cathode – anode gap, a localized discharge channel forms, which may subsequently turn into an electric arc channel if there is enough requisite energy in the primary source.

The time taken by discharge realization ranges into the subnanoseconds. In this case, the similarity law continues to be upheld for gases such as air, nitrogen, argon, helium, oxygen, sulfur hexafluoride, and freon. The theoretical dependence $p\tau = f(E/p)$, which was obtained on the basis of the classic Townsend notions of the exponential growth of the number of electrons and their drift in the electric field, as well as of the potential redistribution in the discharge circuit according to the Kirchhoff law, agreed closely with the experimental data of different authors. This disproves the assertions by several authors that cast doubt on the applicability of Townsend's concept and the validity of using the similarity law for the collisional ionization coefficient α/p as a function of E/p for electric fields $E > 10^5$ V cm^{-1} in an air breakdown.

When there is no external source of initial electrons in a millimeter-long gap, they arrive only from the cathode, primarily due to field emission. The FE current increases due to the increase in the external electric field. In such a discharge, which has been conventionally termed the discharge with one-electron initiation, the similarity law for the time τ is not obeyed. In atmospheric air for $E \approx 10^6$ V cm^{-1}, for instance, the time τ is one order of magnitude longer than in the multielectron initiation. This is due to the deficiency of electrons in the gap as a result of electron self-braking in the avalanche, as well as of the relatively long de-excitation time of excited atoms ($\sim 10^{-9}$ s). The latter has the effect that photons emerge late, which delays the arrival of secondary photoelectrons from the cathode.

In suchlike discharges, the so-called runaway electrons start playing an important role. For high E/p, the energy gained by an electron per unit path length exceeds the energy imparted in inelastic collisions, and the electron passes to the regime of continuous acceleration. At the cathode, these electrons are emitted from separate micropoints due to the FE current when the electric field is around 10^6 V cm^{-1}. In particular, in atmospheric air discharges, these electrons produce diffuse channels formed by jets of REs. Subsequently, as a result of the explosion of the micropoints and the emergence of explosive electron emission, in their place there emerge discharge channels with cathode spots.

Runaway electrons are detected by either the X-ray radiation from the anode or directly by a Faraday cup if the anode is made of a thin foil. For a cathode, use is made of a point, a blade, or rolled foil, whose surfaces have micropoints. In this case, the RE current may range from several to several hundred Amperes. This current is inherently pulsed, with the pulse duration of the order 10^{10} s or less. The most probable source of REs is the FE current from the micropoints on the cathode before the FE turns into the explosive electron emission. The energy required for the manifestation of the runaway effect is gained by the electrons in the cathode region due to the high electric field arising from the electric field nonuniformity in the cathode region. We referred to this nonuniformity as the macrononuniformity, to distinguish it from the microninonuniformity due to the micropoints.

After a lapse of time τ, the current in the gap begins to increase and the voltage across the gap begins to decrease. The instant of the onset of fast current increase and voltage decrease is believed to be the upper bound of the time interval τ. The voltage decrease has two stages: fast and slow. The fast stage duration is characterized by a time θ that obeys the similarity law $p\theta = F(E/p)$. The experimentally determined time θ was proven to be consistent with the estimates made in

the framework of the avalanche electron multiplication theory in the case of multielectron initiation. The stage of slow decrease is then also described by the theory of multi-avalanche electron multiplication and obeys the similarity law. For one-electron initiation, the similarity law also applies to the time θ, which is equal to the same time in the multielectron initiation. This is an indication that during the time τ, an accumulation of free electrons in the gap occurs, in particular, due to the RE current and the photoemission from the cathode, followed by an increase in the current during one avalanche generation to a value such that a rapid voltage decrease occurs. However, the slow decay stage in this case proceeds much faster than for the multielectron initiation. It is caused by the production of a large number of discharge channels between the cathode and the anode.

There are two types of a microwave discharge: single-pulse and periodic-pulse. In the former case, the discharge formation time was shown to obey the similarity law, i.e., the time τ depends only on E/p. In the latter case, the breakdown electric field intensities obey the similarity laws for pulse repetition rates 100 Hz and higher.

References

1. Engel A, Steenbeck M *Elektrische Gasentladungen, Ihre Physik und Technik* Vols 1, 2 (Berlin: J. Springer, 1932, 1934) [Translated into Russian (Moscow – Leningrad: ONTI Gl. Red. Obshchtekh. Lit i Nomografii, 1935, 1936)]
2. Brown S C *Basic Data of Plasma Physics* (Cambridge, Mass.: MIT Press, 1959) [Translated into Russian (Moscow: Gosatomizdat, 1961)]
3. Korolev Yu D, Mesyats G A *Avtoemissionnye i Vzryvnye Protsessy v Gazovom Razryade* (Field-Emission and Explosive Processes in a Gas Discharge) (Novosibirsk: Nauka, 1982)
4. Francis G *Ionization Phenomena in Gases* (New York: Butterworths Sci. Publ., 1960) [Translated into Russian (Moscow: Atomizdat, 1964)]
5. Lozanskii E D, Firsov O B *Teoriya Iskry* (Spark Theory) (Moscow: Atomizdat, 1975)
6. Phelps A V *Phys. Rev.* **117** 619 (1960)
7. Bortnik I M *Fizicheskie Svoistva i Elektricheskaya Prochnost' Elegaza* (Physical Properties and Electric Strength of Sulfur Hexafluoride) (Moscow: Energoatomizdat, 1988)
8. Guseva L G *Zh. Eksp. Teor. Fiz.* **32** 993 (1957) [*Sov. Phys. JETP* **5** 812 (1957)]
9. Dikidzhi A N, Klyarfel'd B N *Zh. Tekh. Fiz.* **25** 1038 (1955)
10. Guseva L G, Klyarfel'd B N *Zh. Tekh. Fiz.* **24** 1168 (1954)
11. Kreindel' Yu E *Plazmennye Istochniki Elektronov* (Plasma Sources of Electrons) (Moscow: Atomizdat, 1977)
12. Korolev Yu D, Mesyats G A *Fizika Impul'snogo Proboya Gazov* (The Physics of Pulsed Gas Breakdown) (Moscow: Nauka, 1991)
13. Sanders F H *Phys. Rev.* **44** 1020 (1933)
14. MacDonald A D *Microwave Breakdown in Gases* (New York: Wiley, 1966)
15. Raizer Yu P *Lazernaya Iskra i Rasprostranenie Razryadov* (Laser-Induced Spark and Discharge Propagation) (Moscow: Nauka, 1974) [Translated into English: *Laser-Induced Discharge Phenomena* (New York: Consultants Bureau, 1977)]
16. Loeb L B *Fundamental Processes of Electrical Discharges in Gases* (New York: J. Wiley & Sons, 1939) [Translated into Russian (Moscow – Leningrad: Gostekhizdat, 1950)]
17. Allen K R, Phillips L *Electrical Rev.* **173** 779 (1963)
18. Schade R *Z. Phys.* **108** 353 (1938)
19. Meek J M, Craggs J D *Electrical Breakdown of Gases* (Oxford: Clarendon Press, 1954) [Translated into Russian (Moscow: IL, 1960)]
20. Przybylski A *Z. Phys.* **168** 504 (1962)
21. Teich T H *Z. Phys.* **199** 378 (1967)
22. Kremnev V V, Mesyats G A *Zh. Prikl. Mekh. Tekh. Fiz.* **1** 40 (1971)
23. Mesyats G A, Bychkov Yu I, Kremnev V V *Usp. Fiz. Nauk* **107** 201 (1972) [*Sov. Phys. Usp.* **15** 282 (1972)]
24. Babich L P, Loĭko T V, Tsukerman V V *Usp. Fiz. Nauk* **106** (7) 49 (1990) [*Sov. Phys. Usp.* **33** 521 (1990)]
25. Raether H *Z. Phys.* **117** 524 (1941)
26. Raether H *Electron Avalanches and Breakdown in Gases* (Washington: Butterworths, 1964)
27. Fletcher R C *Phys. Rev.* **76** 1501 (1949)
28. Sroka W *Phys. Lett.* **14** 301 (1965)
29. Legler W *Z. Phys.* **143** 173 (1955)
30. Wagner K *Z. Naturforsch. A* **19** 516 (1964)
31. Mesyats G A, Doctoral Thesis (Tomsk: Tomsk Polytechnic Institute, 1966)
32. Kunhardt E E, Byszewski W W *Phys. Rev. A* **21** 2069 (1980)
33. Stankevich Yu L, Kalinin V G *Dokl. Akad. Nauk SSSR* **177** 72 (1967) [*Sov. Phys. Dokl.* **12** 1042 (1968)]
34. Mesyats G A, Bychkov Yu I *Zh. Tekh. Fiz.* **37** 1712 (1967) [*Sov. Phys. Tech. Phys.* **12** 1255 (1968)]
35. Goodal D, Hancocs R, in *Proc. of the VI Intern. Conf. on Phenomena in Ionized Gases, Paris, France, 1963* (Eds P Hubert, E Crémieu-Alcan) (Paris, 1963)
36. Mesyats G A, Bychkov Yu I, Korolev Yu D, in *Proc. of the X Intern. Conf. on Phenomena in Ionized Gases, Oxford, England, 1971* (Oxford: Parson, 1971) p. 168
37. Dickey F R (Jr.) *J. Appl. Phys.* **23** 1336 (1952)
38. Felsenthal P, Proud J M *Phys. Rev.* **139** A1796 (1965)
39. Mesyats G A, Bychkov Yu I, Iskol'dskii A M *Zh. Tekh. Fiz.* **38** 1281 (1968) [*Sov. Phys. Tech. Phys.* **13** 1051 (1969)]
40. Krompholz H et al., in *Proc. of the 15th IEEE Intern. Pulsed Power Conf., Monterey, 2005* (Piscataway, NJ: IEEE) (to be published)
41. Korolev Yu D et al. *Zh. Tekh. Fiz.* **49** 410 (1979)
42. Dokhodov V Kh, Zhukov V A *Zh. Tekh. Fiz.* **51** 1858 (1981)
43. Vorob'ev V V, Iskol'dskii A M *Zh. Tekh. Fiz.* **36** 2095 (1966) [*Sov. Phys. Tech. Phys.* **11** 1560 (1967)]
44. Tarasenko V F, Yakovlenko S I *Usp. Fiz. Nauk* **174** 953 (2004) [*Phys. Usp.* **47** 887 (2004)]
45. Mesyats G A, Proskurovskii D I *Pis'ma Zh. Eksp. Teor. Fiz.* **13** 7 (1971) [*JETP Lett.* **13** 4 (1971)]
46. Mesyats G A *Pis'ma Zh. Tekh. Fiz.* **1** 885 (1975) [*Sov. Phys. Tech. Phys. Lett.* **1** 385 (1975)]
47. Baksht R B, Korolev Yu D, Mesyats G A *Fiz. Plazmy* **3** 652 (1977) [*Sov. J. Plasma Phys.* **3** 369 (1977)]
48. Mesyats G A *Ektony v Vakuumnom Razryade*: *Proboi, Iskra, Duga* (Ectons in a Vacuum Discharge: Breakdown, Spark, Arc) (Moscow: Nauka, 2000) [Translated into English: *Cathode Phenomena in a Vacuum Discharge*: *the Breakdown, the Spark, and the Arc* (Moscow: Nauka Publ., 2000)]
49. Gurevich A V *Zh. Eksp. Teor. Fiz.* **39** 1296 (1960) [*Sov. Phys. JETP* **12** 904 (1961)]
50. Noggle R C, Krider E P, Wayland J R *J. Appl. Phys.* **39** 4746 (1968)
51. Babich L P *High-Energy Phenomena in Electric Discharges in Dense Gases*: *Theory, Experiment, and Natural Phenomena* (ISTC Science and Technology Series, Vol. 2) (Arlington Va., Futurepast, 2003)
52. Mesyats G A et al. *Pis'ma Zh. Tekh. Fiz.* **32** (1) 35 (2006) [*Tech. Phys. Lett.* **32** 18 (2006)]
53. Gould L, Roberts L W *J. Appl. Phys.* **27** 1162 (1956)
54. Mesyats G A *Pis'ma Zh. Eksp. Teor. Fiz.* **83** 21 (2006) [*JETP Lett.* **83** 19 (2006)]